Outdoor performance of PV modules made by Solarge

M.H. Ossaili

solarge

TU Delft Delft University of Technology

Outdoor performance of PV modules made by Solarge

by

M.H. Ossaili

to obtain the degree of Master of Science
at the Delft University of Technology,
to be defended publicly on Thursday November 17, 2022 at 15:00 PM.

Student number:	4977971	
Project duration:	February 1, 2022 – November 17, 2022	
Thesis committee:	Dr. ir. P. Manganiello,	TU Delft, Assistant Professor & Supervisor
	Dr. ir. M. van den Donker,	Solarge, External expert & Daily supervisor
	Prof. Dr. A. Weeber,	TU Delft, Professor
	Dr. A. Shekhar,	TU Delft, Assistant Professor

This thesis is confidential and cannot be made public until

Preface

This master thesis remarks the end of a long chapter and the start of a new one. The interest in climate change and renewable energy already exist since I was a little boy. All choices I made since high school lead to my dream to work in renewable energy. In the first year of my bachelor, 2013, in mechanical engineering at De Haagse Hogeschool, I knew I wanted to do the Master in Sustainable Energy Technology in Delft. After all these years of hard working, I can finally say that I achieved my goal.

The aim of my thesis project was to find and compare the thermal- and electrical behaviour for the polymer modules, made by Solarge, and glass modules. This project was versatile, making it interesting and a joy to perform this research. Solarge provided all help and necessities I needed to execute this research. Because of their flexible attitude, I was able to design the mounting system and install the PV modules that I needed. I would like to thank Solarge for giving me the chance to grow my knowledge, not just on the theoretical side of PV technology, but also on the perspective regarding the installation of a PV system and analysing its data.

More specific, I would like to thank Harm Visscher and Jeroen Pijs for all their effort during the installation of the mounting system and PV modules. Without them, the installation would have been much tougher. Also Simona Villa played an important role in the installation of the system, but also helped me with reading the data. Thanks a lot for being available for any data related questions. I would also like to thank Katarina for being a listening ear as office buddy. In addition, I would like to thank Prof. Arthur Weeber and Dr. Aditya Shekhar for being part of my graduation committee.

I would like to thank two people the most regarding this Thesis work. Dr. Patrizio Manganiello and Dr. Menno van den Donker. Both started and ended with so much enthusiasm, passion an joy. Every meeting with the three of us was not just a review session, but also an inspiration to watch two persons talking with so much passion about what they do. I have learned a lot from your knowledge and insight in the way you analyse the PV system.

Finally, I would like to thank Sarah, my parents, sister, family and my friends for their support and for always being there for me. Their unconditional support was a privilege to have.

Delft, November 2022

Abstract

After signing the Paris climate agreement, countries were bounded to reduce their carbon emissions and invest in renewable electricity. PV modules are one of the solutions to generate renewable electricity. Rapid increase in installed PV can also be seen in The Netherlands, where PV systems are installed on rooftops of all sorts of buildings. However, not all buildings can carry the weight of PV strings that make use of conventional glass-based PV modules. Lightweight PV modules,as the one manufactured by the company Solarge, offer a solution to the weight limitations. The weight reduction in the PV modules manufactured by Solarge is obtained by the use of an innovative polymer, replacing the conventional glass frontsheet and PVF-PET-PVF backsheet. However, such a module build-up can affect the operating conditions of the PV cells from both a thermal perspective and an optical perspective.The aim of this thesis project is to analyse and compare the thermal behaviour and electrical performance of polymer-based PV modules, as developed by Solarge, and conventional glass-based PV modules through outdoor experiment in order to quantify differences in performance and identify the root cause of such differences. Furthermore, the thermal behaviour and electrical performance of polymer-based PV modules with white- and black backsheets are also studied.

First, an experimental setup was designed and installed. The PV modules selected for the installation considered four types of PV modules: (1) half-cut-cell-based polymer PV modules, (2) half-cut-cell-based glass PV modules, (3) full-cell-based polymer PV modules with a white backsheet, and (4) full-cell-based polymer PV modules with a black backsheet. All PV modules had a pre-installation check through electroluminescence and I-V measurement under a sun simulator.

The first thermal- and electrical behaviour comparison was performed for the polymer- and glass modules over the period of 1 June till 30 September. It was found that increasing wind speed affects the cell temperature of glass modules more compared to the polymer modules. On the other hand, the level of irradiance affects more the cell temperatures of the polymer modules. Overall, it was found that the solar weighted average cell temperature was higher for the polymer modules, [39.1 - 39.3]$^{\circ}C$, compared to the glass modules, [36.9 - 37.2]$^{\circ}C$. Regarding the electrical behaviour, it was found that the mean energy yield of the polymer modules was 4.69% lower compared to the mean energy yield of the glass modules. Also the the glass modules had a higher daily performance ratio, 91.5 - 92.2%, compared to the polymer modules, [87.5 - 87.7]%. Part of the difference in energy yield and performance ratio origins in the higher cell temperature for the polymer modules. However, further analysis of the operating currents of the PV modules showed that an important part of such a difference in energy yield and performance ratio is likely linked to higher optical losses in the polymer-based PV module.

The second thermal- and electrical behaviour comparison was performed for the white backsheet- and black backsheet polymer modules over the period of 1 June till 30 September. It was found that increasing wind speed affects the cell temperature of black backsheet polymer modules more compared to the white backsheet polymer modules. On the other hand, the level of irradiance affects the cell temperatures of the white backsheet- and black backsheet polymer modules with a comparable heating rate. Overall, it was found that the solar weighted average cell temperature was comparable with [38.3 - 38.7]$^{\circ}C$ for the white backsheet polymer modules and [38.1 - 38.7]$^{\circ}C$ for the black backsheet polymer modules. Regarding the electrical behaviour, it was found that the mean energy yield of the white backsheet polymer modules was 1.54% higher compared to the mean energy yield of the black backsheet polymer modules. Also, the white backsheet polymer modules had a higher daily PR, [87.7 - 89.1]%, compared to the black backsheet polymer modules, [86.8 - 87.8]%. Small differences were found also when comparing PV modules' currents and voltages. However, all these differences are within measurement error, therefore it is not possible to conclusively identify whether they are mostly due to thermal or optical effects.

Contents

List of Figures

List of Tables

Nomenclature

Abbreviations

AOI	Angle of Incidence
$c-Si$	crystalline Silicon
DC	Direct Current
DHI	Direct Horizontal Irradiance
EL	Electroluminescence
EY	Energy Yield
GHI	Global Horizontal Irradiance
$I-V$	Current-Voltage
MPP	Maximum Power Point
$MPPT$	Maximum Power Point Tracking
NTC	Negative temperature coefficient
PR	Performance Ratio
PV	Photovoltaic
STC	Standard Test Conditions
SWA	Solar Weighted Average

Symbols

EY	Energy Yield [kWh/kWp]
I	Current [A]
I_{MPP}	Current at MPP [A]
I_{SC}	Short-circuit current [A]
I_{STC}	Current characterized under STC [A]
P	Power [W]
P_{MPP}	Power at MPP [W]
P_{STC}	Power characterized under STC [W]
PR	Performance Ratio [%]
R	Resistance [Ω/m]
T_{rel}	Relative cell temperature [°C]
V	Voltage [V]
V_{MPP}	Voltage at MPP [V]
V_{OC}	Open-circuit Voltage [V]
V_{STC}	Voltage characterized under STC [V]

1 Introduction

1.1. PV market

Climate change is a known problem for some decades, but the urge of attacking this problem with actions like investments in sustainable energy was not there. Even after the Paris climate agreement, countries did not directly choose for a rapid change. However, countries that did sign the Paris climate agreement made targets for 2020, 2030 and 2050. The closer a Country came to 2020 and the more visible climate change, the more investments were done in sustainable energy. This can be seen in the increase of installed renewable capacity [1]. Also the development curve of the renewable energy technologies helped to convince politicians, companies and consumers to invest. One of the markets that is increasing very fast is the photovoltaic (PV) market. The installed PV capacity is also growing rapidly, as in the Netherlands where the installed capacity increased by 33.9% in 2021 [2]. There are PV systems installed on residential roofs, in the industry, integrated in buildings and even open fields are used.The acceleration of the PV development and installation seems to be limitless. However, not every roof is built to carry the weight of PV modules. This is especially the case for industrial-, agricultural- and distribution center buildings. The largest obstacle for that in the Netherlands origins from constructional weakness, where the rooftops are not able to carry heavy loads. Research, lead by TKI Urban Energy, investigated utility buildings that have constructional limitations for carrying weight. They looked to 4 type of buildings, namely: Distribution centres, agricultural buildings, (not heavy) industrial buildings and old buildings that are in public or commercial use [3]. These 4 type of buildings were sorted into three catagories:

- No constraints: No or small constructional adaptations needed to install PV system
- Small constraint: A few constructional adaptations needed to install PV system
- Heavy constraints: A lot of constructional adaptations needed to install PV system

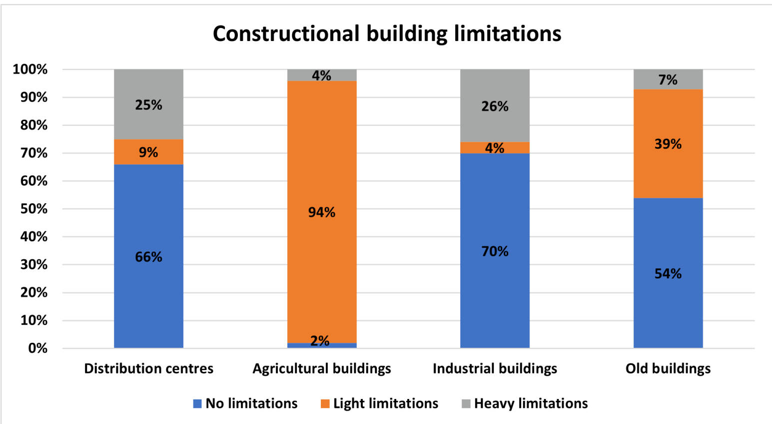

Figure 1.1: Constructional building limitations found in building types presented in 3 categories [3]

As Figure 1.1 shows, there is a large range of buildings that need first adaptations, before the PV system can be installed. This is exactly where the potential lies for the lightweight solar modules in the market. Using lightweight modules would mean that owners of buildings with constructive limitations do not need to invest in constructive roof reinforcements.

1.2. Lightweight PV modules

The development of solar cell technology is rapidly increasing in type, materials, efficiency and production techniques. Focusing on the market of lightweight PV modules, it can be seen that the biggest development in weight reduction comes from the replacement of glass and a metal frame with polymer based materials. The variety of glass free modules is also large, since they vary in type of cell, like thin-film amorphous silicon (a-Si) or crystalline-silicon (c-Si), but also in flexibility and backsheet materials. HyET Solar is a company that develops thin-film applications that can be used for rooftop PV generation. The PV modules that HyET produces are glass free and weight around 0.78 kg/m^2 [4], where a conventional glass frontsheet module weights between 12 and 16 kg/m^2 [5]. However, the fabrication of thin-film cells is more complex than the c-Si cells, making the fabrication harder and more expensive to scale up which results in a higher cell price at the moment [6]. There are also PV modules that use c-Si cells, but are glass free, have the same flexibility like the HyET solar modules and need to be glued as well. Sunman PV modules are an example of this type of PV modules. Their modules consist of c-Si solar cells that are laminated on polymer based front and backsheets, creating the flexibility of the module. In the lightweight market, Solarge came with a new product compared to the thin-film modules and flexible c-Si modules. The PV modules, made by Solarge, are consist of a polymer based front- and backsheet, but still contain the strength of a conventional glass frontsheet PV module with metal frame. This creates the benefit that conventional mounting systems and market leading solar cells can still be used. The Solarge SOLO module weights 5.5 kg/m^2, which is around 50% less weight than a conventional glass module.

1.3. Solarge

As explained in section 1.2, the PV modules, made by Solarge, are designed to be an lightweight alternative for conventional modules and not an alternative for flexible lightweight modules. Solarge originated from a collaboration of companies that exchanged knowledge. This collaboration resulted in a establishment of Solarge in 2018. The Solarge module consists of fibre reinforced polymers and special developed polymers from SABIC [7]. These polymers are developed in such way that they can replace the glass frontsheet and metallic frame, while maintaining strength and safety. Furthermore, the polymers are also considered to be easy recyclable materials, which reduces the carbon footprint of the modules. The difference between polymer PV modules, made by Solarge, and conventional glass PV modules can be seen between Figure 1.2, showing the polymer materials used by Solarge, and Figure 1.3, showing the conventional glass PV module material layers. The solar cells can be considered to be similar, but the Solarge layout differs from not containing a glass frontsheet, PVF-PET-PVF backsheet and metallic frame.

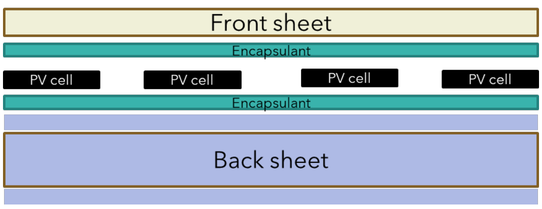

Figure 1.2: Layout polymer PV module made by Solarge

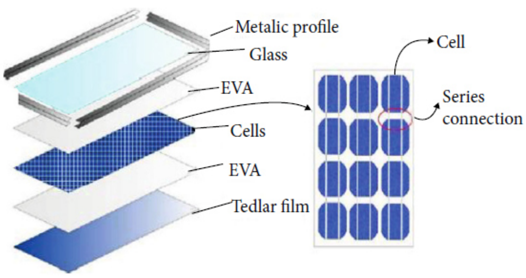

Figure 1.3: Layout conventional glass PV module [8]

Table 1.1 displays the parts of the PV modules that are not similar to each other. The density of the materials clarify the weight reduction of 50% by the polymer PV modules, made by Solarge, compared to a conventional glass-based module. The polymers, used by Solarge, have densities that are less than half of the density of the conventional materials.

Module type	Module Part	Material	Density $[kg/m^3]$
Glass module	Frontsheet	Glass	2500 [9]
	Backsheet	PVF-PET-PVF	1700 [10]
	Frame	Aluminum	2700 [11]
Solarge module	Frontsheet	Innovative polymer	905 [12]
	Backsheet	Innovative polymer	207 [13]
	Frame	-	-

Table 1.1: Material densities

1.4. Aim of the Thesis

The previous sections explained the need for PV modules, especially the need for lightweight modules. Their potential can be found in the unused large rooftops that have constructional limitations. Although, polymer PV modules, made by Solarge, can be considered as lightweight modules, they should be compared with conventional glass modules. Section 1.3 explained the density difference between polymer PV modules made by Solarge and conventional glass PV modules. However, the impact of the polymer materials on the performance of the PV cells compared to conventional glass frontsheet modules with the same type of PV cells is not yet fully understood. The different materials, compared to glass PV modules, that cover the PV cells in a PV module, made by Solarge, will have a different impact on the thermal behaviour of the module, thus the cell temperature which affects the electrical performance. Therefore, this thesis will focus on the following questions where the sub-questions provide answers to the main questions.

1. How does the innovative polymer-based PV module technology made by Solarge perform in outdoor conditions both electrically and thermally?
   (a) What is the influence of materials used for the polymer PV modules, made by Solarge, on the cell temperature?
   (b) What are the energy yield and performance ratio of polymer PV modules made by Solarge?
2. How does the performance of polymer PV modules compare to conventional glass-based PV modules?
   (a) What is the influence of materials used for the conventional glass-based PV modules on the cell temperature?
   (b) What are the energy yield and performance ratio of glass-based PV modules?
   (c) How does modules made by Solarge perform compared to glass-based PV modules?
3. How does the performance of polymer PV modules with a white backsheet compare to polymer PV modules with a black backsheet?

Scope The energy yield of PV modules can be influenced by many factors that are directly influencing the module or a PV system as a whole. Therefore, the scope of this project is as follows:

- The thermal behaviour of the module, influencing the cell temperature, will be researched. The thermal effect of the junction box or wires will not be researched.
- The optical behaviour will not be researched, due to thesis time limitations.

1.5. Thesis outline

Now that the reader has been introduced to the scope and background of the research topic, chapter 2 provides a more thorough theoretical background. The design, installation and used equipment of the used measurement setup is described in chapter 3. After, the results of the data analysis regarding the performance of the modules made by Solarge are discussed and compared with the performance of the conventional glass modules. These results will be presented in chapter 4. Finally the conclusion and recommendations will be discussed in chapter 5.

2 Literature Study

In chapter 1 the growing PV market with the potentials for lightweight PV modules were presented. PV modules made by Solarge are considered as lightweight PV modules that could benefit from the potential rooftops with constructional limitations. Solarge makes use of innovative polymers that reduces the weight of the module, but the remaining question is how this polymer impacts the thermal behaviour of the PV module. The thermal behaviour will influence the cell temperatures and thus influence the electrical performance. This research includes measurements and data analysis that allows quantitying and understanding needed to answer the influence of the polymers on the thermal behaviour of the PV module, and its effect on the overall PV module performance.

In chapter 1 the PV market has been explained and the position of Solarge in this market. On the other hand, the objectives for this research are set, showing that the performance and thermal behaviour of the polymer PV modules, made by Solarge, need to be researched. Experimental measurements and a thermal model will lead to results that can explain the performance and thermal behaviour. However, to understand what the data is telling, the theoretical knowledge needs to explained first. Starting with understanding the modules that are used and their differences.

2.1. Electricity and heat generation inside a PV cell

The creation of electrical energy generated by a PV module starts all with light energy, photons, radiated by the sun. Each photon has it's own energy level, depending on its wavelength, and reaches the surface of the PV module within a different angle. Once the photons reach the surface of the PV module, they will be reflected, transmitted or absorbed by the frontsheet. The photons that are transmitted will then reach the cell surface and will then, depending on their wavelength, be absorbed or transmitted. This wavelength dependency comes from the bandgap energy of a solar cell. Every cell type will have different configurations and materials that define the cell. The most common material used for solar cells and also the material used for modules made by Solarge is crystalline Silicon, c-Si, that has a bandgap of around 1.12eV [14].

Figure 2.1 shows how the photon energy depends on the wavelength, which will result in either absorption or transmission of the photon. The lower the wavelength, the larger the photon energy. Photons with a wavelength above the maximum required wavelength of the bandgap energy have not enough energy to excite an electron from the valence band to the conduction band and will be transmitted through the material. When a photon has an equal- or higher energy than the bandgap energy, it is able to excite an electron, charge carrier, from the valence band to the conduction band.

Photons that have a higher energy level than the bandgap energy will excite an electron deeper into the conduction band where it will then release the excess energy in the form of heat. Increasing temperature has a decreasing effect on the bandgap, meaning that photons with lower energy levels than the original required energy level are able to excite electrons, causing an increase in mobile charge carriers.

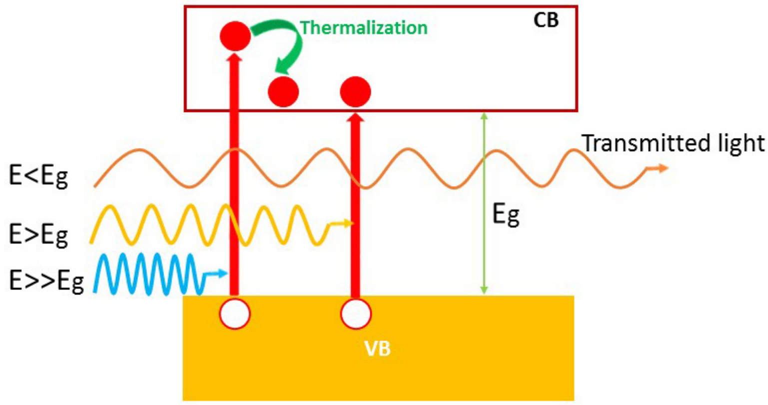

Figure 2.1: Relation of photon energy with bandgap energy [15]

2.2. Electrical parameters of PV modules

2.2.1. Standard Test Conditions (STC)

The PV market consists of many companies and laboratories that produce different PV technologies, considering cell or module technologies, and are located all around the world. The performance of different technologies are then compared to track new developments, but also to prove the commercial value of the technology compared to conventional technologies in the PV market. Therefore, Standard Test Conditions (STC) are implemented as the standard indoor measurement conditions under which the performance of a PV module must be evaluated. The STC are characterised as follows [14]:

- **Irradiance:**$1000W/m^2$
- **Spectrum:** $AM1.5$
- **Cell temperature:** $25°C$

Under the described characteristics of STC, PV modules perform at the highest achievable maximum power point(mpp). The rated power that is measured is then called the STC power,P_{STC}. The maximum power point is defined by two important parameters that are also measured under STC. Namely, the short-circuit current, I_{sc}, and open-circuit voltage, V_{oc}. The I_{sc} and V_{oc} define the behaviour as well as the performance of the module. Therefore, subsection 2.2.2 provides more background information.

2.2.2. Short circuit current and open circuit voltage

The flow of excited electrons per unit area are defined as the current density and is at its maximum when defined as short-circuit current density, J_{sc}. The maximum voltage is called the open-circuit voltage, V_{oc}, and is measured when the short-circuit current density is zero.

The open-circuit voltage can be described as Equation 2.1 and shows a dependency on the short-circuit current density, J_{SC}, but also the dark current density,J_0.

$$V_{OC} = \frac{nk_BT}{q} ln(\frac{J_{SC}}{J_0}) \tag{2.1}$$

The increasing temperature resulting in a decreasing bandgap energy cause an increase of the short-circuit current density, since the flow of electrons increased. However, the increase in extra hole- and electron charge carriers increases the intrinsic carrier concentration, n_i. Equation 2.2 shows that dark current density is squared related to the intrinsic carrier concentration, since an increased concentration results in an increased recombination rate. Equation 2.2 shows the this relationship, where B_J is the constant that is temperature independent.

$$J_0 = q{n_i}^2(\frac{D_N}{L_N N_A} + ln\frac{D_P}{L_P N_D}) = B_J{n_i}^2 \tag{2.2}$$

As the temperature increase will increase J_0 more significant than J_{SC}, the V_{OC} will decrease with increasing temperature. Therefore the heavier effected V_{oc} shifts the maximum power point, reducing the output power of the cell and therefore reducing the efficiency of the cell, as Figure 2.2 shows.

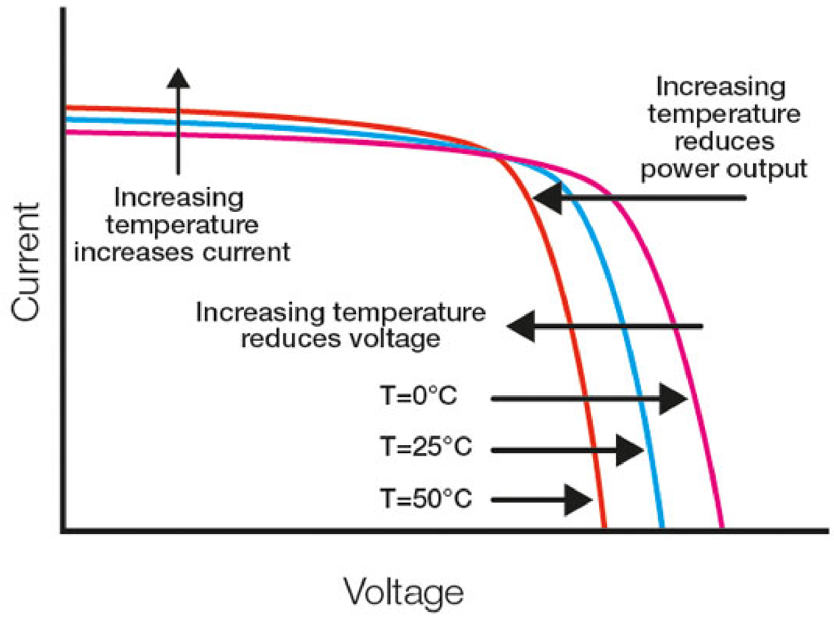

Figure 2.2: Temperature effect on I-V curve [16]

2.2.3. Resistance

Generation and transport of electricity comes with resistance. Series- and shunt resistance effects the performance of solar cells and eventually modules.

Series resistance is caused by three mechanisms. These are the movement of current through the base and emitter of the cell, the contact resistance between the metal contact and the silicon and the resistance of the top and rear metal contacts [14]. Shunt resistance, also called leakage currents, is characterized by current through local defects in the junction or due to shunts at the edges of the solar cell . In general the aim regarding resistance is to have series resistance as low as possible, while shunt resistance needs to be as high as possible [14].

Increasing temperature will decrease the bandgap of the cell and allow more photons to excite electrons. This will increase the short circuit current, but the increased concentration of charge carriers will also increase the recombination rate. Therefore the saturation current will increase even more strongly, which will result in an reduction of the open-circuit voltage. Based on research, it can be found that the series resistance in a cell increases with temperature, while the shunt resistance decreases with temperature [17] [18]. This behaviour results in a decrease in the Fill Factor and open-circuit voltage, which directly results in power loss.

Series resistance also contains the metal contact resistance. Regarding conventional crystalline silicon solar cells, these are the front- and back metal contacts. Regarding the front contacts, there are the fingers and busbars. Equation 2.3 displays the dependency of the resistance on the metal contact parameters. Longer contacts as well as decreasing width and height result in higher resistance, where as an increasing width will increasing shading losses.

$$R = \frac{\rho * L}{W * H} \tag{2.3}$$

The power loss created in the metal contacts can be calculated by Equation 2.4. The power loss is equal to the current squared multiplied by the series resistance, also called contact resistance.

$$P_{Loss} = I^2 * R \tag{2.4}$$

Based on Equation 2.4 scientists and the industry developed half-cut cells. These are basically full cells of, for example, c-Si, but then cut in half. This halves the current and therefore reduces the current that flows through the busbars. This results in a decreased power loss. An additional advantage of half-cut cells is the minimized shading loss. This is the result of more rows for half-cut cell modules, with 3 rows on each half of the module, instead of 3 rows in total over the length of the module. When shade covers half of the module, then the half-cut cell module is still able to produce with half of the module and bypassing the shaded part of the module [19].

2.2.4. Energy yield

Energy yield is one of the two performance parameters that will be used in this research. The main focus of this research is the performance of the PV modules. Therefore, the DC energy yield is used, which calculates the ratio of instantaneous PV power by the PV power generated during standard test conditions [20].

$$EY_{DC} = \frac{\int_{t_0}^{t_1} P_{DC}\, dt}{P_{stc}} \tag{2.5}$$

The energy yield, described in Equation 2.5, is given in the units [kWh/kWp], where the measured power in [kW] becomes [kWh] after integration with time. The stc power is measured during an I-V measurement and is a constant value that is used in the calculation.

2.2.5. Performance ratio

The performance ratio (PR) is the second performance parameter that will be used in this research. This parameter is one of the most used performance metrics, that measures how effectively a module converts irradiance into energy [21]. The irradiance that is used for the PR is the plane-of-array irradiane. This is the irradiance measured with an pyranometer that is mounted in the same tilt angle as the installed PV modules. The plane-of-array irradiance can therefore be seen as the irradiance that the PV modules receive.

$$PR = \frac{\int_{t_0}^{t_1} P_{DC}(t)\, dt}{\int_{t_0}^{t_1} G(t)\, dt} * \frac{G_{STC}}{P_{STC}} \tag{2.6}$$

The performance ratio, described in Equation 2.7, makes use of the measured DC power and measured plane-of-array irradiance. The use of the integral converts the power and irradiance into energy. The performance ratio is a metric that quantifies losses that are not related to irradiance. However, the loss factor does include module temperature as well, while module temperature is dependent on the weather and thus irradiance. Therefore, the weather-corrected performance ratio is created [21].

$$PR = \frac{\int_{t_0}^{t_1} P_{DC}(t)\, dt}{\int_{t_0}^{t_1} P_{STC}(\frac{G(t)}{G_{stc}})(1 - \frac{\delta}{100}(T_{cell_avg} - T_{cell}(t))\, dt} \tag{2.7}$$

where δ is the temperature coefficient for power [$\%/^{\circ}C$], T_{cell_avg} is the average cell temperature [$^{\circ}C$] over a year of data and $T_{cell}(t)$ is the measured cell temperature [$^{\circ}C$] at time t. The weather-corrected performance ratio, described in Equation 2.7, will take out seasonal fluctuations and show more effectively the losses that are related to the module itself instead of losses caused by the weather.

2.2.6. Temperature coefficients

Key electrical parameters have been mentioned and common performance metrics, used in the PV research, are mentioned. The short-circuit current and in particular open-circuit voltage are influenced by the cell temperature. The reaction of current and voltage to temperature directly influence power output of the cell. The relation of current, voltage and power with cell temperature are therefore expressed in temperature coefficients and expressed as follows:

- **Temperature coefficient current:**$\alpha = [\%/^{\circ}C]$
- **Temperature coefficient voltage:**$\beta = [\%/^{\circ}C]$
- **Temperature coefficient power:**$\gamma = [\%/^{\circ}C]$

The temperature coefficients that are presented in datasheets of PV modules define the percentage change with respect to a STC cell temperature of 25$°C$, under $1000W/m^2$ and $AM1.5$.

2.3. Heat transfer physics

section 2.1 and section 2.2 described how electricity is generated, but also how the generation and transport of electricity can create energy loss in the form of heat. Besides, the effect of rising cell temperatures also contribute to power loss and indirect to heat generation. However, the generated heat will not stay at the same position, but will be transferred to different layers of the module. Weather conditions also play a role in cooling or heating the module, as well as transferring heat. In general heat transfer consists of three forms, namely radiation, convection and conduction. These work in different ways and influence the module in different ways.

2.3.1. Radiation

As section 2.1 starts, the sun radiates light energy to the earth. This radiation contains energy in the form of photons and if referred to as irradiance. Materials that do not convert these photons into electricity can absorb the photons as heat. On the contrary, the module will radiate heat in the form of electromagnetic waves or photons. This depends on the emissivity of the module. The heat transfer by radiation can be calculated with Equation 2.8:

$$Q_{radiation} = \varepsilon\sigma({T_M}^4 - {T_{amb}}^4) \tag{2.8}$$

where ϵ is the emissivity, σ is the Stefan-Boltzmann constant ($\simeq$ $5.67x10^{-8}W/m^2K^4$, T_M is the module temperature and T_{sky} is the ambient temperature.

2.3.2. Convection

Convection is the heat transfer from a surface to a moving fluid. The moving fluid is, in the case of a pv module on the roof, air flowing on the top and bottom surface of the module. The flow of air can be distinguished into two flow types, namely free- and forced air flow. The free flow is caused by temperature differences, influencing the fluid density. Forced flow is based on the fluid flow that is caused by external forces, which is wind in the case of a PV module. Further distinction is made between laminar and turbulent flows. The laminar flow is dominant at low velocities while turbulent flow is stronger at high velocities. The heat transfer by convection can be calculated with Equation 2.9:

$$Q_{convection} = h_c\Delta T = h_c(T_M - T_a) \tag{2.9}$$

where h_c is the convective heat transfer coefficient [W/m^2K], T_M is the module temperature [k] and T_a is the air temperature. In this formula, it is the convective heat transfer coefficient that gets influenced by the flow conditions.

2.3.3. Conduction

The last heat transfer type is the conduction of heat. Thermal conduction is the heat transfer created by the temperature difference with one or more materials. This is defined by Fourier's law of heat conduction, stating that in a homogeneous substance, the local heat flux is proportional to the negative of the local temperature gradient [22]. The heat transfer by conduction can be calculated with Equation 2.10:

$$Q_{conduction} = -k\frac{dT}{dx} \tag{2.10}$$

where k is the thermal conductivity [W/mK], T is the local temperature [k] and x is the coordinate in the flow direction [m].

2.3.4. Thermal material properties

The heat is transferred in the three previous explained ways, via or within a material. Each material has different properties that effect the rate heat is transferred. These material specific properties will be further explained.

Thermal conductivity
Thermal conductivity describes how well a material is able to conduct or transfer thermal energy. It describes the rate of heat flow across a temperature gradient within a material. High thermal conductivity means that a large amount of heat can quickly be transferred over a distance. On the other hand, low thermal conductivity will result in none or low amount of heat that can be transferred through a material.

(Specific) heat capacity
Heat capacity describes the quantity of thermal energy required to increase a unit temperature of a material. "Specific" refers to the heat capacity per unit mass of a material [23]. Low specific heat capacity can be described as a low amount of heat that is required to increase the temperature of the material. High specific heat capacity can be defined as a large amount of heat is necessary to increase the temperature of the material.

Emissivity
The emissivity, also called emittance, is related to the radiation that a material emits. Only a perfect emitter, a blackbody, has an emissivity of 1.0. The lower the emissivity, the less radiation will be emitted.

Density/thickness
The thermal properties discussed above all depend on the dimensions of the materials. Therefore the density and thickness of materials are important as well.

2.3.5. Surface color in relation to thermal behaviour

The emissivity, mentioned in subsection 2.3.4, described that a black body is the perfect emitter. The black body, or black surface, is by definition a surface that absorbs all incident radiation and reflects none [22]. As a result, black surfaces emit most radiation, compared to all other type of surfaces. Based on this information, the hypothesis is created that a black surface absorbs more heat compared to a white surface. In perspective of this Thesis, the hypothesis is that the polymer PV module with a black backsheet will have a higher module temperature compared to a polymer PV module with a white backsheet.

2.4. Glass frontsheet PV module: materials and properties

There are today various types of PV modules on the market, as explained in chapter 1. Nevertheless, the conventional glass PV module with crystalline silicon PV cells is still the major type module that is sold on the market and the components that are used are overall the same as well [24].

Conventional glass frontsheet PV modules that dominate the PV market, contain overall the same configuration of layers, but differ in materials types and especially in cell types. Going into detail for every specific material is out of the scope of the research, so therefore the most common materials will be discussed.

Frontsheet: Glass is used as a frontsheet and provides in the first place protection for the solar cells. Parallel to protection, the frontsheet needs to transmit as much of the incident light as possible to the cell. The type of glass, used in conventional PV modules, has a reduced iron level resulting in reduced light absorption loss [14]. The transmittance of soda-lime glass is around 90% and when antireflective coatings are used, this can even rise to 98% [25].

Encapsulants: The solar cells are placed between two layers of ethylene-vinyl-acetate (EVA) encapsulant layers. This sandwich will be heated, changing the EVA structure and enables that the the layers will stick together [14]. Encapsulants have the main function of electrical insulation, protecting the PV cell and metalic contacts from moisture and environmental particles.

Backsheet: The backsheet of conventional glass PV modules is made of layers PVF-PET-PVF. The PVF stands for polyvinyl fluoride, which is mainly produced by DuPont who gave PVF the name Tedlar. PVF is functional for withstanding vapours and is resistive against weathering. PET is the short name for polyethylene terephthalate and functions as an electrical isolator. The overall function of the backsheet is to protect the module from humidity and withstand stresses. The current market shows also a small market section using glass backsheets, but for this research the focus is set on the conventional modules with PVF-PET-PVF backsheets.

Frame: The metal frame is often made of aluminium and creates mechanical stability. The metal frame enables installers to mount the modules on specific installation systems.

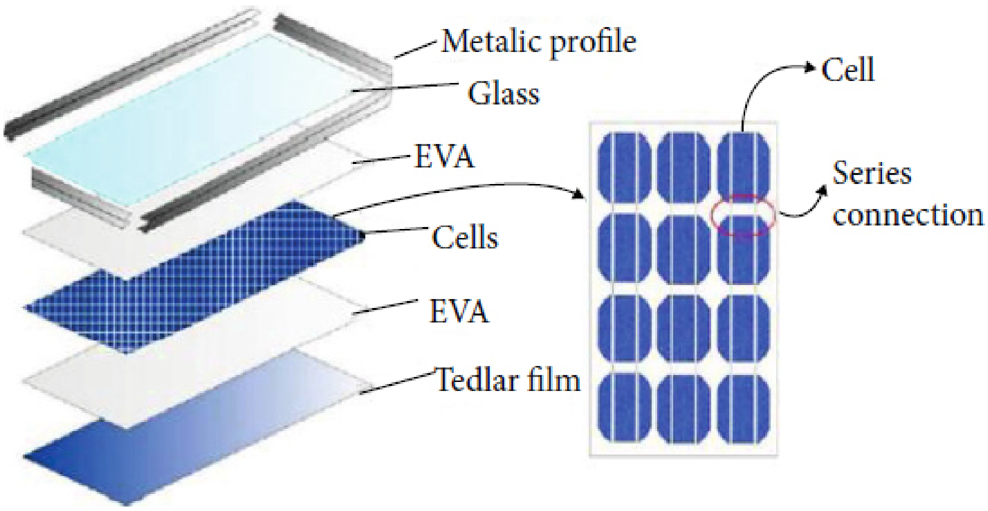

Figure 2.3: Layout conventional glass frontsheet PV module [8]

All the conventional glass PV module components combined create the module composition as Figure 1.3 shows. The list and figure do not show electrical components like the junction box and wires, but that is out of the scope since the major difference between conventional glass- and polymer (Solarge) PV modules is within the modules.

Table 2.1: Materials Conventional glass frontsheet PV module

Parts of conventional PV module	Thickness [mm]	Thermal conductivity [W/mK]	Density kg/m^3	Specific heat capacity [J/kgK]
Glass [26]	3.2	1.8	3000	500
Ecanpsulant EVA [26]	0.58	0.35	960	2090
Solar Cell	0.19	60		
Ecanpsulant EVA [26]	0.58	0.35	960	2090
PVF-PET-PVF backsheet [26]	0.34	0.2	1200	1250
Aluminium frame [22]		168	2790	883
Total thickness	4.89*			

*Thickness considering cell position from top to bottom, so no frame included in this position.

The conventional PV module, consisting of a glass frontsheet and TPT backsheet, have the parameters as displayed in Table 2.1.

2.5. Polymer PV module: layout and materials

The layout and commonly used materials of conventional glass PV modules are described, as are the functions of the materials to the module. Polymer PV modules, made by Solarge, show overall the same layout, but use different materials, that will be further explained in this section. Starting from the top layer towards the bottom layer.

Frontsheet: The frontsheet used by Solarge is made of an innovative polymer. The used frontsheet functions, similar to glass, as the protection layer for the solar cells, while transmitting the incident light.

The polymer used by Solarge is made in co-operation with Sabic, that keeps the exact recipe secret. The frontsheet transmits 89% of its light. This is around 1% less transmission compared to soda-lime glass without AR-coating, but 9% less compared to soda-lime glass with AR-coating [27].

Encapsulants: The encapsulant for polymer PV modules made by Solarge are just like the conventional glass PV modules placed between the frontsheet and PV cell as well as between the PV cell and backsheet.

Backsheet: The backsheet used by Solarge, is made of several polymer layers, containing different added materials. This sandwich panel consists of two thin fibre reinforced polymer layers with a core in-between. The materials used for the backsheet are chosen such, that it keeps the stiffness and strength needed for the forces applied under outdoor conditions. The backsheet is a composite of several layers and materials of which exact thermal characteristics are unknown. One of the main questions of this research is to find the thermal behaviour of the front- and backsheet.

The layout of a Solarge module differs from the commercial PV modules. It differs in having not a glass frontsheet and not a PVF-PET-PVF backsheet. The Layout consists of the following layers:

Table 2.2: Materials Solarge module

Part of Solarge module	Thickness [mm]	Thermal conductivity [W/mK]	Density kg/m^3	Specific heat capacity [J/kgK]
Polymer frontsheet	0.45	0.14	905	1580
Encapsulant	0.45	0.14		
Solar Cell	0.19	60		
Encapsulant	0.45	0.14		
Backsheet	12.2		265	
Total thickness	13.74			

3
Outdoor experimental setup

In this chapter, the outdoor experimental setup, used to collect performance data of the polymer modules made by Solarge and glass modules made by Evocells, is treated. The setup was realized together with TNO and it is located on the rooftop of faculty Vertigo, which is part of the Technical University of Eindhoven. This roof consists of multiple different cabins that have different rooftop designs, providing the ability to experiment different PV modules. The motivation and requirements for the outdoor experimental setup will be discussed in section 3.1. Then the design of the setup and installation of the modules will be briefly explained in section 3.2. Finally, the collection of data will be clarified in section 3.3.

3.1. Motivation and requirements

The main question for this research is to analyse the outdoor performance of the polymer modules made by Solarge and glass based modules and understand the reason of any measured differences. The best understanding of outdoor performance is to actually install the modules outdoors and measure the behaviour. The collected data can then display the thermal- and electrical behaviour, that lead to answers that can clarify the main questions. Chapter 2 explained in detail the differences in materials between the polymer modules and glass-based modules. Solarge investigated their theoretical thermal performance by external parties, that executed the calculations by software. However, performance of the modules that experience real-time weather conditions describe a far more realistic and accurate behaviour. Outdoor conditions are, unlike indoor measurements, uncontrollable with stable- and unstable periods that can be seen over days, but even within minutes. The uncontrollable weather conditions cause uneven distributed weather conditions over the PV mdoule that can cause different temperatures within the PV module. Besides weather conditions, the design of the PV module and materials used in the PV module play a role in the heat transfer as well. Therefore, the placement and number of sensors used to measure the theraml behaviour of the modules need to be decided and planned before the installation.

Requirements The experimental setup is all about answering the research questions. Therefore, the requirements of the design are that the PV modules and equipment that will be installed directly contribute to answering the research questions. Another requirement is related to the reduction of measurement uncertainty. This means that at least two PV modules of each type need to be installed and at least two thermal sensors need to be placed on the PV module to measure the cell temperature. Two module comparisons will be done during this research. One is between the polymer PV modules and glass PV modules, both containing half-cut c-Si cells. The second comparison is done with polymer PV modules with a white backsheet and polymer PV modules with a black backsheet, both containing full c-Si cells. chapter 2 explained the difference between full cells and half-cut cells, which can lead to different thermal- and electrical behaviours. Besides that, cells with different efficiencies and power output, need extra normalisation calculations to be compared.

3.2. Design and installation of the system

The modules that are used will be placed on the roof of a small cabine at the Technical University of Eindhoven(TU/e). The TU/e made it available for companies and organizations to test different module types and mounting systems in association with TNO. The roof that will be used has a width of 6.0 meter and length of 6.3 meter. The biggest part of the roof is available for this experiment and has no limitations regarding the design of the installation.

3.2.1. Type of modules and positioning

The performance of polymer modules need to be compared with the performance of the glass modules. Therefore, Solarge made two polymer PV modules with 120 half-cut cells that are compared with two glass PV modules with 108 half-cut cells [28]. The cells are from the exact same manufacturer and are the same type of cells. This needs to provide the best comparison between glass modules and polymer PV modules. Besides the polymer-glass comparison, there is also a comparison between black- and white backsheets for polymer modules made by Solarge. The same type of full cells are used, namely the M10 MONO PERC crystalline-silicon cells.

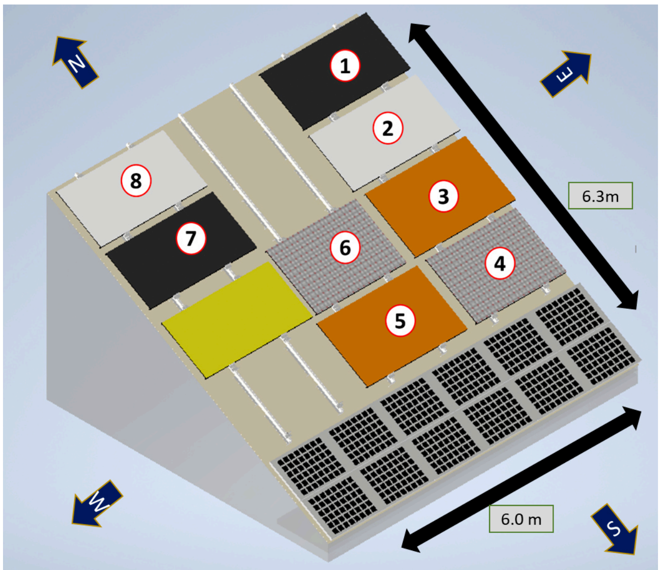

Figure 3.1: Designed experimental setup with PV modules positioned on the 3D drawn cabin. The modules face to the South.

Figure 3.1 shows in the first two rows from the bottom the 6 special designed modules by Solarge for Sabic. Sabic needs to be able to experiment with the modules for their research, so therefore it is decided that the modules, used for this research, are placed above the two bottom rows, such that shading by adjustments of the first two rows are minimalized. Furthermore the modules are positioned such that they all have comparable environmental conditions. The wind and temperature at the edge can differ from a position in the middle of the roof surface. To reduce uncertainty in the data, it is chosen to position one polymer half-cut cell module (orange) and one glass half-cut cell module at the side (red dotted area) and one of both modules in the middle. Regarding the black backsheet polymer module and white backsheet polymer module, they are positioned both at the sides, because there is a free space left.

Module naming

The modules that will be installed as numbered in Figure 3.1 receive a short label name. The original label names, used by TNO said something about the position of module on the roof. The new label names differ from the old names, but re-used the ascent numbering order of the two modules. The list of names and positions, as assigned in Figure 3.1, can be found in Table 3.1.

Module type	Research label name	*Plot label name	Module number
Polymer module (Solarge)			
Full cell White backsheet	Polymer-F-White(1)	P-F-W(1)	8
Full cell White backsheet	Polymer-F-White(2)	P-F-W(2)	2
Full cell Black backsheet	Polymer-F-Black(1)	P-F-B(1)	1
Full cell Black backsheet	Polymer-F-Black(2)	P-F-B(2)	7
Half-cut cell	Polymer-H(1)	P-H(1)	3
Half-cut cell	Polymer-H(2)	P-H(2)	5
Glass module			
Half-cut cell	Glass-H(1) 3	G-H(1) 3	6
Half-cut cell	Glass-H(2) 4	G-H(2) 4	4

*Plot label name only used in case of lacking space within plot

Table 3.1: Module label names and positions

3.2.2. Measurement instruments

The measurement data of the module performance and weather conditions are retrieved by various instruments. Each instrument execute a specific measurement that will be collected and stored on cloud performance dashboard platform. The weather measurement instruments consists of the following

Figure 3.2: DNI,DHI and GHI measurement instruments

Figure 3.3: High sensitivity anemometer for wind speeds

Figure 3.4: Pyranometer to measure Plane-Of-Array irradiance

Figure 3.2,Figure 3.3 and Figure 3.4 present the instruments, used to measure the weather conditions. Figure 3.2 presents a so called all-in-one device containing a pyrheliometer to measure DNI and a shaded pyranometer to measure the DHI. Based on the DNI and DHI, GHI can be calculated by the software, Figure 3.3 presents a high sensitivity anemometer that is capable to measure wind speed and wind direction. Figure 3.4 presents a pyranometer, manufactured by Eko instruments [29], fixed to the cabin on which the PV modules are installed. The pyranometer is mounted in the same angle as the PV modules are. In this way, the general plane-of-array irradiance is measured. This is comparable to the irradiance that is received by the PV modules.

3.2.3. Temperature sensors and positioning

The measurements that are done consists of thermal, electrical and environmental measurements.The thermal behaviour will be defined by the data that is obtained from temperature sensors. The sensors that are used for cell temperature measurement are NTC thermocouple sensors. NTC (negative temperature coefficient) sensors are made of semiconductor materials that allow current to flow. The lower the temperature, the higher the resistance in the sensor. NTC sensors are very sensitive to temperature change, making it an accurate measurement device [30]. The cell temperature are the most important with respect to the performance of the module. In chapter 2, it was explained that increasing cell temperatures result in reduced V_{OC} that leads to lower power output of the module. The closer the sensor is placed to the cell, the more accurate the temperature is measured. Therefore, the original idea was to laminate a thermocouple between the encapsulant and the backsheet of the polymer modules. Thermocouples are very thin temperature sensors that economically and practically feasible. Eventhough the fact that the sensor diameter is 0.25mm, this would still give an offset below the cells, increasing the chance of cell cracks. Another risk of this idea originates from the production process where Solarge is bending the module edges. This process and the transportation of the modules can lead to sensor damages, since the thermocouples are fragile. Once the sensor is laminated, replacement is not possible anymore.

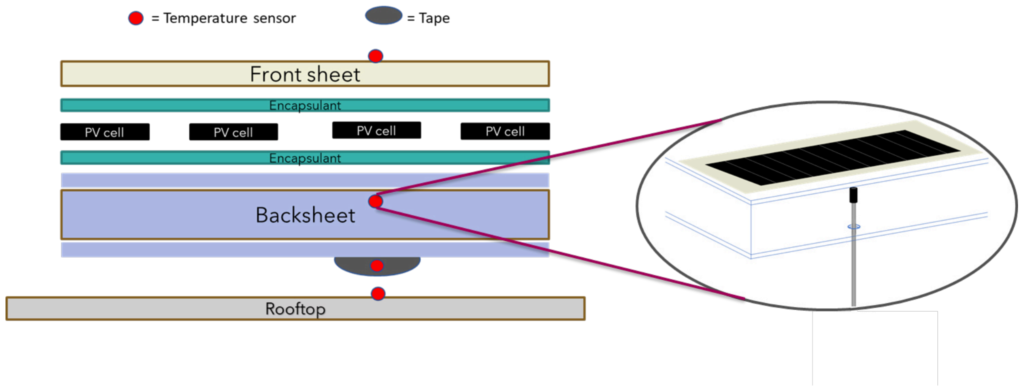

Figure 3.5: Sensor positioning within backsheet of polymer modules to measure cell temperature

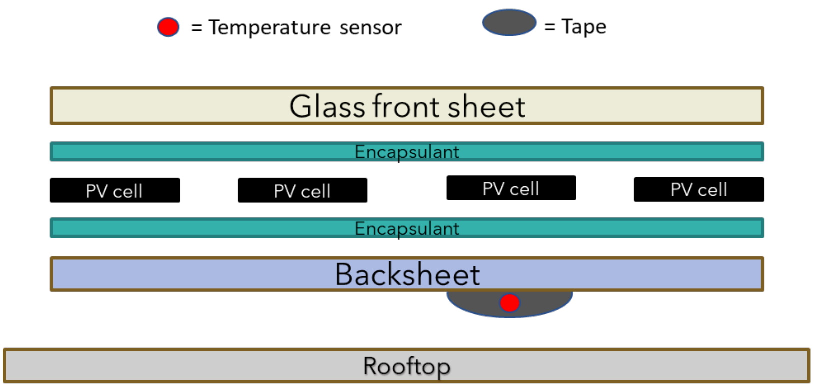

Figure 3.6: Sensor positioning on backsheet of glass modules to measure cell temperature

The risks that came with the lamination of thermocouples, lead to alternative positioning of the sensors. Figure 3.5 displays one polymer half-cut cell module that carries more temperature sensors, compared to the other polymer modules. Nevertheless, the sensor positioned in the core of the backsheet is the consistent position used to measure the cell temperature for all polymer modules. In this case the sensor is positioned in the backsheet and placed against the top skin of the backsheet. At this position, the sensor will be 0.95mm below the cell with the encapsulant and backsheet skin in between.

The outdoor thermal behaviour is the unknown, because of the use of different materials within different layers. In section 2.3 it was explained how heat is transferred to-, from- and through the module. When all material specifications, such as thermal properties, are known, then heat transfer calculations can be easier made. However, the backsheet and polymers with different additives contain many unknown thermal properties. Therefore, one polymer module that will be compared to glass-based modules is chosen to have more sensors, that can leas to insight in the heat transfer through the module. The glass module contain a PVF-PET-PVF backsheet with a thickness of just 0.34mm and encapsulant of 0.58mm. Taping the thermal sensor at the backsheet creates a distance of 0.92mm between the sensor and the PV cell. Figure 3.6 presents the positioning of the sensor to the backsheet. Positioning of the sensor closer to the cell is not possible from a practical perspective, increasing the risk of irreversible damage.

3.3. Data

The experimental setup is meant to collect weather- and performance data to answer the research questions. After clarifying the design of the installation as well as the used equipment for the measurement, the specified data collection needs to be described. Table 3.2 lists all data that is collected at the setup.

Weather data		Performance data	
- GHI	- Plane-of-array irradiance	- DC power	- DC energy
- DNI	- Wind speed & direction	- DC current	- Module/cell temperature
- DHI	- Sun altitude & azimuth	- DC voltage	
- Humidity	- Ambient temperature		

Table 3.2: All collected data from the experimental setup

The weather data is measured by installed measurement equipment located on the rooftop. The plane-of-array irradiance is measured by an installed pyranometer that is mounted to the roof of the modules, in the same angle as the modules. The wind-, humidity- and ambient temperature data is measured at a weather station, that is located at the rooftop. All weather data is measured every minute at the exact same time, at exactly zero seconds of a minute. The electrical data is measured via a Solaredge inverter that is randomly measuring all electrical values of a module at a random moment. The random measurement moment results in a measurement point that is taken at a random minute as well as random seconds. This means that the electrical data is not measured at the same time as the weather data, meaning that extra filters and interpolation is needed to extract the most reliable data.

3.4. I-V measurement and pre-installation check

The selected modules that are described in subsection 3.2.1 were first checked, to determine the status and conditions of the modules. The pre-installation check consists of two steps that are performed indoor. The first step is execution of electroluminescence (EL) , in a dark cabin. The flash, created by the camera, lights up the PV cells that clearly show cells that are intact, cracks or dark spots on the PV cells. The second step is the indoor I-V measurement that determines the performance of the PV module under STC.

Figure 3.7: Ecoprogetti Ecosun sun simulator I-V measurement device, used to generate the module performance under STC

Figure 3.7 presents sun simulator, of the manufacturer Ecoprogetti, used for I-V measurements, equipped at Solarge. The PV module is placed on the black line of wheels, electrical cable are connected to the device and carefully rolled into the measurement area inside the unit. Inside, the AM 1.5 spectrum is imitated with lamps and a level of irradiance close to 1000 W/m^2 is re-created. The ambient temperature is equal to the room temperature that is measured. The software of the I-V measurement unit is able to convert the measurements into the actual performance that the PV module would generate under STC. Finally, the results of the I-V measurement are presented with showing the P_{STC}, I_{mpp}, V_{mpp}, I_{sc} and V_{ov}. The

Module name	$P_{STC}[W]$	$V_{mpp}[V]$	$I_{mpp}[A]$	$V_{oc}[V]$	$I_{sc}[A]$
Polymer-F-White(1)	355.1	40.1	8.86	48.8	9.4
Polymer-F-White(2)	355.7	40.1	8.86	48.8	9.41
Polymer-F-Black(1)	353.6	40.3	8.78	48.7	9.35
Polymer-F-Black(2)	353.1	40.2	8.79	48.7	9.33
Polymer-H(1)	404.4	34.1	11.85	41	12.5
Polymer-H(2)	404.4	34.1	11.87	41	12.49
Glass-H(1)	385.3	30.6	12.61	37.1	13.49
Glass-H(2)	388.7	30.7	12.67	37.2	13.32

Table 3.3: Obtained indoor I-V measurement performance data under STC

3.5. Realisation of setup

The setup was realized after the mounting systems was designed and materials were ordered. Together with TNO, collegues from Solarge and myself the installation of the mounting system as well as the modules was realized. After mounting the mounting system, the PV modules were able to be installed as planned and designed in Figure 3.1. The glass modules had temperature sensors double taped at the backsheet.

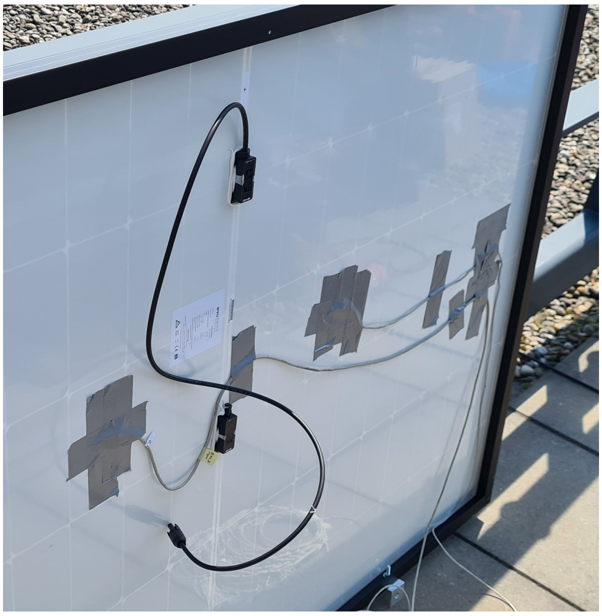

Figure 3.8: NTC sensor taped at the glass module backsheet

The polymer PV modules made by Solarge needed an extra step to place the NTC sensors. Figure 3.9 displays the steps of sensor positioning. First a hole had to be drilled in the backsheet to place the sensor below the top skin of the backsheet. Then glue was injected into the hole and immediately the NTC sensor was pushed into the hole. After some minutes, the glue dryed and the sensor was in position. The last step was to double tape the first part of the sensor that sticked out of the hole, to make sure that the sensor stayed in place and is protected from potential temperature influence leaking through cracks in the glue.

(a) NTC sensor hole drilled in polymer backsheet

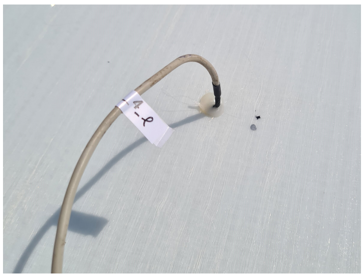

(b) NTC sensor glued in drilled hole of polymer backsheet

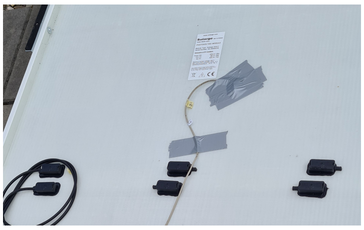

(c) NTC sensor double taped at the back as extra stability and protection

Figure 3.9: NTC sensor placement in polymer backsheet

After the placement of the sensors, the modules were installed one by one, resulting in the setup shown in Figure 3.10a. The type of modules are shown in Figure 3.10b, presenting the same order as designed beforehand. The ”Yellow module” that was placed is out of the scope for this research and was used by Solarge. Since it is on the picture, this needs to be clarified, but will not be mentioned further in the report.

(a) All modules installed on the roof including pyranometer at the right side of the cabin.

Polymer-F-White (1)	-	Polymer-F-Black (1)
Polymer-F-Black (2)	-	Polymer-F-White (2)
Yellow module	Glass-H (1)	Polymer-H (1)
-	Polymer-H (2)	Glass-H (2)

(b) Layout of placed module type

Figure 3.10: (a) The PV modules are installed on the cabin located at the TU/e. The modules are installed in the layout of figure (b). On the right side of the cabin the pyranometer is visible. This pyranometer measures the plane-of-array irradiance.

3.6. Conclusion

In this chapter the motivation and requirements of the experimental setup were explained and the design for the setup was presented. The measurements need to provide the research outdoor data that can answer questions related to the thermal- and electrical performance of the modules. The NTC sensors play an important role in answering thermal questions, by measuring the cell temperatures during outdoor operations. The sensors were placed as close to the cell as possible, by double taping the sensors on the back of the glass PV modules and by putting the sensor in a hole, drilled in the Solarge backsheet. Furthermore, it was listed which data will be collected at the experimental setup that can be used for answering the research questions.

4

Results and analysis

The performance- and weather data obtained from the outdoor measurement setup, explained in chapter 3, was analysed and results will be elaborated in this chapter. The performance results of the polymer- and glass module comparison will be explained in the following structure. The thermal behaviour of the modules will be shown and compared, based on the irradiance- and wind effects on the cell temperature. Subsequently, the electrical performance of the modules will be presented and compared. The results of the white- and black backsheet module comparison will be presented in the same order. The short module names are listed in Table 3.1 and used in the plots and results presented in this chapter.

4.1. Validation and uncertainty

In the start of the research, I-V measurements, have been performed for all PV modules at Solarge. It was found, as Figure 4.1 presents, that the power difference between the manufacturer label on the module and the I-V measurement was more or less 4% for the glass module and Solarge white backsheet with full cells. Since the glass modules were brand new and the deviation from sticker and I-V measurement was more or less the same for both type of modules, it was decided to find the stc power of the modules with the measurement data.

4.1.1. STC module power

The stc power of a PV module gives information of the power output at standard test conditions. This means that the module should deliver the maximum power under the following conditions[14]:

- **Irradiance:**$1000W/m^2$
- **Spectrum:** $AM1.5$
- **Cell temperature:** $25C°$

Based on the given conditions filters were implemented to get the best and most suitable data points over the period of 1 June till 30 September. All data-points together should then create a fitted line that shows a stc power rating that comes close to the stc power rating obtained from the I-V measurement. The preparation of the data set and implemented filters will be discussed one-by-by.

Preparation of the data set

The measured data, collected by TNO, was stored in the online monitoring platform Grafana. The dashboard presented all measured data, including weather and electrical data. The electrical data was originally measured by the Solaredge Power optimizers and sent to the online platform of Solaredge. TNO made it possible to display the data in the same dashboard as the weather data and made sure that all data was given in winter time. The collected weather data like (cell) temperatures, irradiance, wind speed and wind direction were all measured with a time stamp of 1:00 minute. However, all Solaredge optimizers measured the electrical data with a random time stamp. This resulted in data points measured at a random minute and random seconds. Measured data showed that within one minute, the weather can change very fast from clear sky to cloudy and back. Consequently, irradiance fluctuates with the sky conditions resulting in changing power outputs. Figure A.1 presents that when power points are aligned with the plane-of-array irradiance at the same minute, the value of power is different. In the first measured moment the irradiance was 1151W/m^2 and the measured power was 319W, while at the second measurement the irradiance was 1174W/m^2 and the measured power was 192W. Normally, an increase in irradiance results in an increase in power, instead the power drops with 127W. It can be seen from the time stamp in the bottom table that the first measured power moment was after five seconds, while the second moment was after 51 seconds. The irradiance at 14:14:00 was 1151W/m^2, while at 14:15:00 the irradiance was just 410W/m^2. This demonstrates that the reduced power output is more related to the irradiance level of one minute later, compared to the minute it was pointed to. Therefore, it was chosen to interpolate the weather data within every minute, such that the measured power is related to a more realistic level of irradiance.

Data filters

After the preparation of the dataset, filters that lead to the best and most suitable stc power points were implemented.

1. Irradiance Under standard test conditions the level of irradiance is set on $1000W/m^2$. The level of irradiance is very dependent on the amount of clouds and the moment of the year related to the angle of the earth and suns position. Because of fluctuating level irradiance, it was chosen to filter power points measured in the irradiance range of $950W/m^2 \leq G \leq 1050W/m^2$.

2. Altitude of the sun Under standard test conditions, the module is placed perpendicular to the light source. This can be transelated to the angle of incidence (AOI) of $0°$. In outdoor conditions, the angle of incidence is dependent on the position of the sun, orientation of the module and the module tilt. The altitude of the sun varies with the season, because of the earth's angle, while the installed modules are facing to the south with a tilt of $35°$. Using data points only at an AOI of $0°$ is impossible, since this happens only twice a year. Based on research an AOI $\leq 15°$ can be taken to have data points as close to the STC values as possible [31]. However, the measured AOI has a period of no data what made to decide to filter based on the altitude of the sun. Therefore, it was chosen to choose a sun's altitude of $\geq 55°$.

3. GHI/DHI The presence of the clouds can best be seen by the ratio of global horizontal irradiance (GHI) divided by the direct horizontal irradiance (DHI). During cloudy days, the ratio is close to one while clear sky conditions give a ratio close to zero. Based on experience of people at TNO, the filter was set on (GHI/DHI)≤ 0.400. This makes sure that a measured power point was not a wrong measurement during a cloudy moment.

4. Wind speed Indoor standard test conditions use wind conditions of $0m/s$. In outdoor conditions, this could only be achieved when the modules are shielded from the wind. Since this is not the case for the used measurement which will always measure wind speed a maximum value had to be chosen. Based on research in outdoor stc temperature coefficients, the filter used for wind speed was set on $\leq 2m/s$ [32].

5. Minimum power level After the implementation of previous filters, there were still some low power outliers that are not correct. Based on iteration, it was chosen to implement a minimum power value. The minimum value for white- and black backsheet polymer modules was set on $250W$, while the minimum for the glass modules and Solarge half-cut cell modules was set on $275W$.

Data processing and analysis

The power points that are left after all data filters are then multiplied with a factor such that the power rating is related to an stc irradiance level of $1000W/m^2$. This was done by dividing $1000W/m^2$ with the interpolated level of irradiance related to the time stamp of the measured power point. The explained calculation can seen in Equation 4.1.

$$P_{corrected} = P_{module} * (1000/G_{measured}) \tag{4.1}$$

where $P_{corrected}$ is the power [W] scaled to $1000W/m^2$, P_{module} is the measured power [W] and $G_{measured}$ is the general plane array of irradiance interpolated to the time stamp of the power measurement. After the multiplication a data set was obtained with power scaled to stc irradiance and interpolated cell temperature at the same measurement time. The selected and scaled data points were then plotted with cell temperature on the x-axis and power on the y-axis. PV module power under standard test conditions require a cell temperature of $25C°$. Therefore, a linear fitted line was taken through the datapoints to a cell temperature of $25C°$. The best outdoor stc power rating difference compared to the stc power of the I-V measurement for all installed PV modules was found between -6% and -10%. Since all possible filters were implemented and the used values were founded, there had to be a loss or uncertainty either at the measurement side, within the PV module or both. Since all PV modules showed a large difference in stc power rating, the loss was searched outside the PV module. The electrical power was measured with the Solaredge power optimizers, which were installed below the roof and inside the cabin. All PV modules were connected with a $4.00mm^2$ PV cable of 15 meters from the PV module to the Solaredge power optimizers inside the cabin. Since 15 meters is a significant length, cable losses were analysed and calculated.

$$P_{loss} = 2 * I^2 * R_{cable} \tag{4.2}$$

where I is the measured DC current [A], R_{cable} is the resistivity of the cable[Ω/m] and the factor 2 is used since every PV module uses 2 cables. The used PV cables origin from the manufacturer Elettro Brescia. The corresponding resistivity for the used cable with $4.00mm^2$ diameter is $0.00509\Omega/m$ [33]. The power loss was first calculated with the measured values of the I-V measurement. The results are presented in Table A.2 and show that two cables reduce the stc power by 3% for the white- and black backsheet polymer PV modules, 5% loss for the Solarge half-cut cell modules and 6% loss for the glass modules. The significant cable loss can therefore explain a part of the lower stc power after the data filtering. This insight lead to the implementation of an extra step related to the power data. The cable power loss was calculated with the measured current, at the specific power point, and added to the measured power. The new calculated power was then corrected with the stc irradiance factor. The obtained data set with new stc power points was also plotted with cell temperature on the horizontal x-axis and power on the vertical y-axis, as shown in Figure A.2 and Figure A.3.

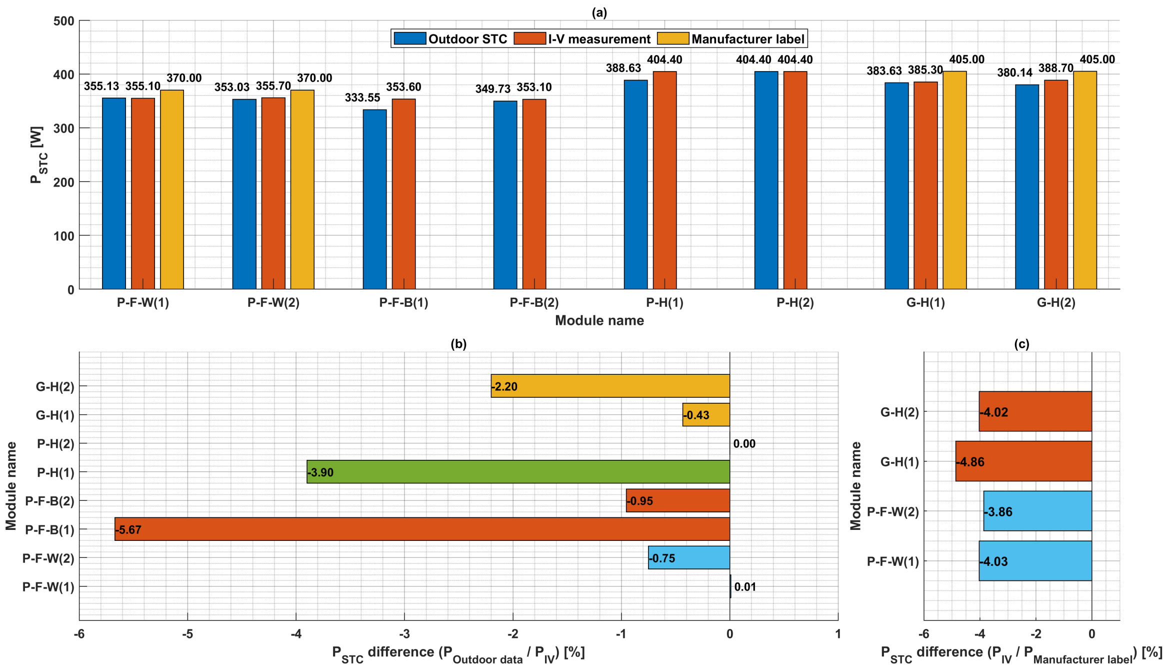

Figure 4.1: (a) Module STC power of manufacturer label, I-V measurement and obtained by outdoor data; (b) Measured difference between the STC power obtained by outdoor data and I-V measurement; (c) Measured difference between the STC power of the I-V measurement and the manufacturer label

Figure 4.1 presents all stc power values that were measured or found by the data fitting. The new outdoor stc power rating compared to the stc power of the I-V measurement for all installed PV modules was found between 0.0% and -5.7%. Eventhough the fact that some outdoor stc values differ almost nothing from the I-V measurement value, there is still a difference being measured that is unexplained. However, not all measured difference can be lead to one exact source. Therefore, uncertainty factors need to be taken into account.

Measurement uncertainty

Data obtained with the outdoor measurement setup, relies on a variety of measurement instruments and the condition of the PV module itself. All collected data is summarised in Table 3.2. The weather data is measured by many measurements instruments like a pyranometer for the plane-of-array irradiance and a high sensitivity anemometer for wind speed. The electrical data is measured in the Solaredge power optimizers, while the cell temperatures are measured with NTC sensors that are connected to a data ticker. All instruments consist a manufacturer standard measurement uncertainty and measurement accuracy degradation over time. Since most of the exact uncertainty values for the specifically used instruments can not be found, results of other research can give answers to a more general uncertainty value for the measured data.

- **Pyranometer [29]:**
  - Directional response - **<10**W/m^2
  - Temperature response - **<1**%
  - Tilt response - **<0.2**%
- **Module performance [34]:**
  - Current/Voltage measurement - **0.05 - 0.2**%
  - Resistance losses - **0.1 - 1.5**%
- **Temperature sensors [34]**
- **Measurement uncertianty:**
  - Single module PR–> 4.5% uncertainty, because you take irradiance as well
  - Comparing PR of multiple modules –> 1.5% uncertainty, e.g irradiance gone because both have same ”problems” or ”benefits”
- **Optics:**
  - Angle-of-Incidence [34] - **0 - 5**%
- **Other losses:**
  - Shading
  - Cable resistance loss

The performance of the PV modules is measured with the Solaredge power optimizer 500. The power optimizer is working with a technique, so called maximum power point tracking (MPPT). MPPT is used to let the PV module function on the maximum power point. The MPP is calculated with Equation 4.3.

$$P_{mpp} = I_{mpp} * V_{mpp} \tag{4.3}$$

With P_{MPP} the power at MPP [W], I_{MPP} is the current at MPP [A] and V_{MPP} is the voltage at MPP [V]. Irradiance as well as the cell temperature affect the I_{MPP} and V_{MPP}. However, irradiance and the cell temperature change over time, shifting therefore I_{MPP} and V_{MPP}. MPPT forces the PV module to operate at MPP to generate maximal power. Voltage is therefore used to force the module to operate at V_{MPP}. The changing weather- and temperature conditions cause a shift in MPP. The power optimizer tries to find the MPP by estimating the P_{MPP} as accurate as possible. However, measurement uncertainties and the estimation around the actual MPP, makes that the MPP that the power optimizer shows will always deviate from the real MPP [14].

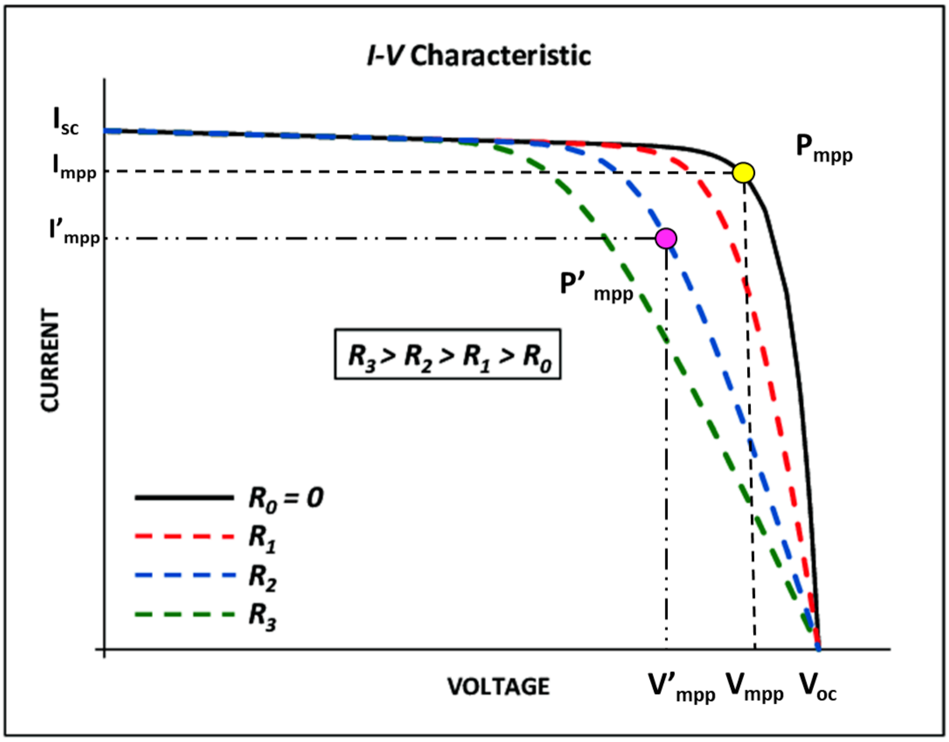

Figure 4.2: I-V curve measured at the PV module without resistive losses and I-V curves including resistive losses.

Figure 4.2 presents several I-V curves where the MPP can be extracted. In the ideal case, the MPP directly measured at the PV module, should match with the yellow dot on the black solid line,I_{MPP} and V_{MPP}. However, the power optimizer measures the MPP values at the end of the cables, including other losses that may occur in optics and measurement uncertainties. In this case I'_{MPP} and V'_{MPP} are measured, that are reduced values resulting in P'_{MPP}. The MPPT done by the power optimizer makes that even in this case one cannot trust 100% the measured P'_{MPP}.

4.2. Outdoor performance of polymer-H & glass-H modules

In chapter 2 it was explained how the polymer- and glass module differ in material types. chapter 3 explained the measurement setup, which made clear that the difference between the polymer-H module and glass-H module was based on the materials used for the front- and backsheet, but not the PV cells. Based on this, the thermal behaviour and electrical performance are further analysed to see the effect of different materials on the performance of PV cells and thus the module. The data, used to analyse, covers the time period between 1 June and 30 September 2022.

4.2.1. Thermal behaviour results

The thermal behaviour of a PV module can be best explained by measuring the cell temperature of the module. The cell performance is influenced by the environmental conditions that directly influence the power output, like the level of irradiance, or indirectly influenced, like the ambient temperature and wind speed. All modules, installed on the roof, have temperature sensors that measure the cell temperature as close as possible to the cell. Before further analysis were done, the temperature sensor data was checked and compared with sensors on the same module. The data showed no divergent behaviour of the sensors compared to the sensors of other modules and were all used for further analysis. The sensor temperatures per module are combined and the average of the measured temperatures is taken.

What cell temperatures do the modules have?

The first understanding of the module behaviour is made by looking closer to the cell temperatures at specific days. These days are based on a clear- or cloudy sky and high or low ambient temperatures. The chosen days from the data set are defined in Table 4.1.

Table 4.1: Weather conditions on specific days

Day charactersitics	Date	Total Gpoa [kWh/m^2]	Average Tamb $[^{\circ}C]$	Average wind speed [m/s]	Average wind direction
Clear sky & high ambient temperature	July 19th	7894	32.9	2.18	East
Clear sky & low ambient temperature	June 14th	8593	18.6	1.12	South-East
Cloudy & high ambient temperature	August 26th	1745	18.6	1.59	South-West
Cloudy & low ambient temperature	June 8th	1860	15.8	2.05	South

Table 4.1 presents a clear difference in measured total irradiance during a clear sky day and cloudy day. The selected days, shown in the table, are then used to show the behaviour of the cell temperatures during the days for the polymer- and glass modules. The temperature sensors are averaged per module and used in the comparison.

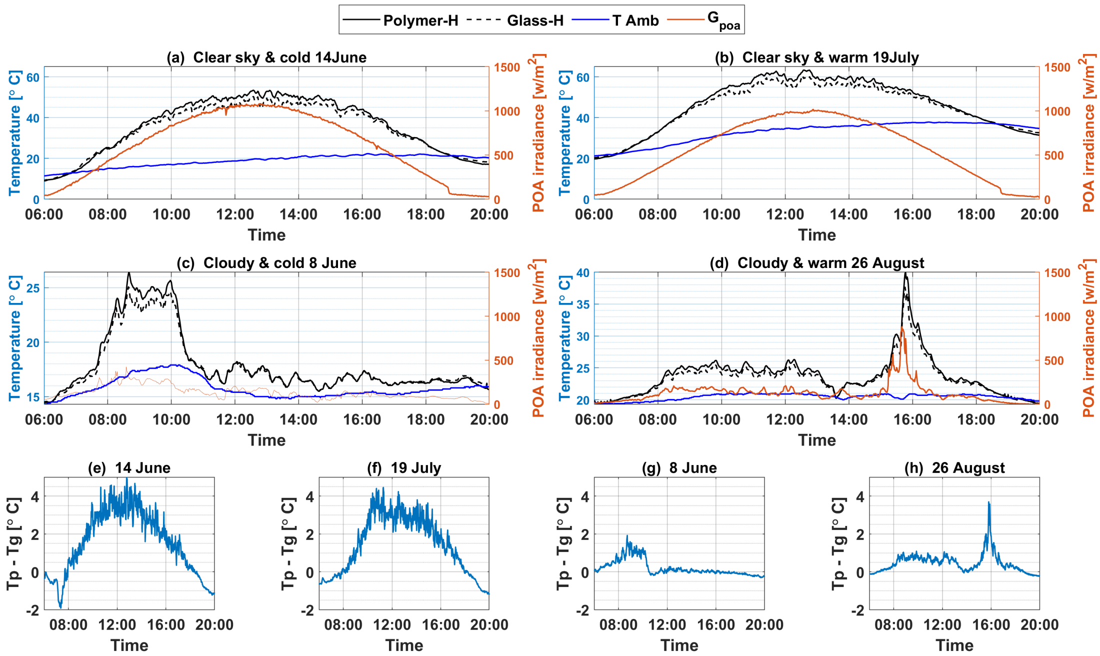

Figure 4.3: Measured Polymer-H and Glass-H PV module cell temperatures, ambient temperature and general plane-of-array irradiane at (a) clear sky & low ambient temperature 14 June; (b) clear sky & high ambient temperature 19 July; (c) cloudy sky & low ambient temperature 8 June; (d) cloudy sky & high ambient temperature 26 August; The measured cell temperature difference between Polymer-H and Glass-H on (e) 14 June; (f) 19 July; (g) 8 June; (h) 26 August

It can be observed from Figure 4.3 that the cell temperatures follow the behaviour of the irradiance that does reach the module, as can be seen by the similarity in trend behaviour. During the selected days, the average cell temperature of the glass module is below the average cell temperature of the polymer modules. The figures in the bottom show, as the level of irradiance increase, the cell temperature difference between polymer- and glass modules increase as well. The cell temperature of the polymer modules respond more significant to the change in irradiance and keeps a higher temperature during steady moments of irradiance. When the level of irradiance reduce, the cell temperature of polymer modules reduce more significant compared to the glass modules. Therefore, the temperature over the entire day will be expressed in the solar weighted cell temperatures. These temperatures are weighted with the general plane of array irradiance.

It can be observed from Table 4.2 that the solar weighted cell temperatures during the selected days with high irradiance, is around two degrees Celsius higher for the polymer modules, compared to the glass modules, while the difference is below one degrees Celsius during low irradiance days. During the 19th of July, the solar weighted ambient temperature is very high, resulting in very high cell temperatures. However, Table A.1 in Appendix A, shows that when the difference between cell- and ambient temperatures are taken, the difference is actually most significant on the 14th of June. This can be an incident, however, irradiance and ambient temperature are the only environmental factors focused on this case. Table 4.1 shows that the average wind speed during the 19th of July was

Date	Ambient [°C]	P-H(1) [°C]	P-H(2) [°C]	P-H [°C]	G-H(1) [°C]	G-H(2) [°C]	G-H [°C]	P-G [°C]
14 June	19.0	43.3	43.7	43.5	41.3	40.8	41.1	2.4
19 July	34.0	53.2	53.7	53.4	52.0	50.3	51.2	2.2
8 June	16.1	19.4	19.3	19.4	19.0	18.9	19.0	0.4
26 August	20.5	26.3	26.2	26.2	24.8	25.9	25.4	0.8

Table 4.2: Solar weighted cell temperatures on the specific days for the polymer-H and glass-H modules

around $1 m/s$ higher compared to the 14th of June. The influence of different wind speeds on the cell temperature of a PV module will therefore be analyzed in more detail. The influence of wind speed is shown, based on 3 days in a row that show stable irradiance, while having varying wind speeds.

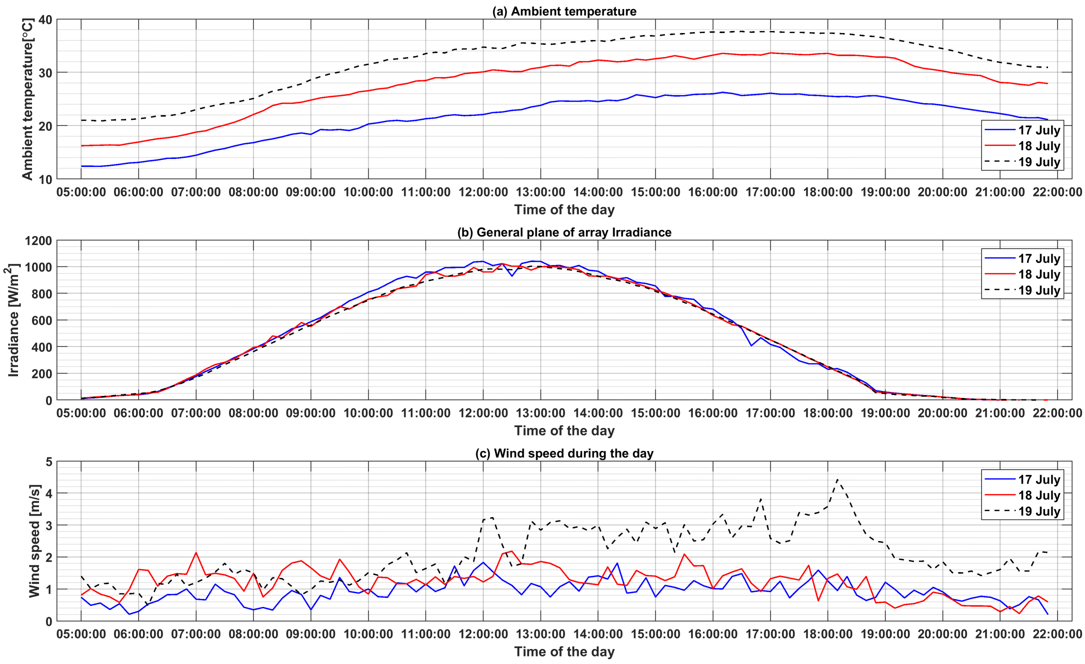

Figure 4.4: Weather conditions on 17, 18 and 19 July with (a) Ambient temperature during the day; (b) General plane-of-array irradiance during the day; (c) wind speed during the day

Figure 4.4 presents the weather conditions during the 17th, 18th and 19th of July. The ambient temperatures differ much between the days, while the irradiance is overall the same, with the exception of the 17th of July between 9:30 and 12:00. The wind speed differs most on the 19th of July during the afternoon with 1 to 2 m/s higher wind speed difference compared to the 17th and 18th of July.

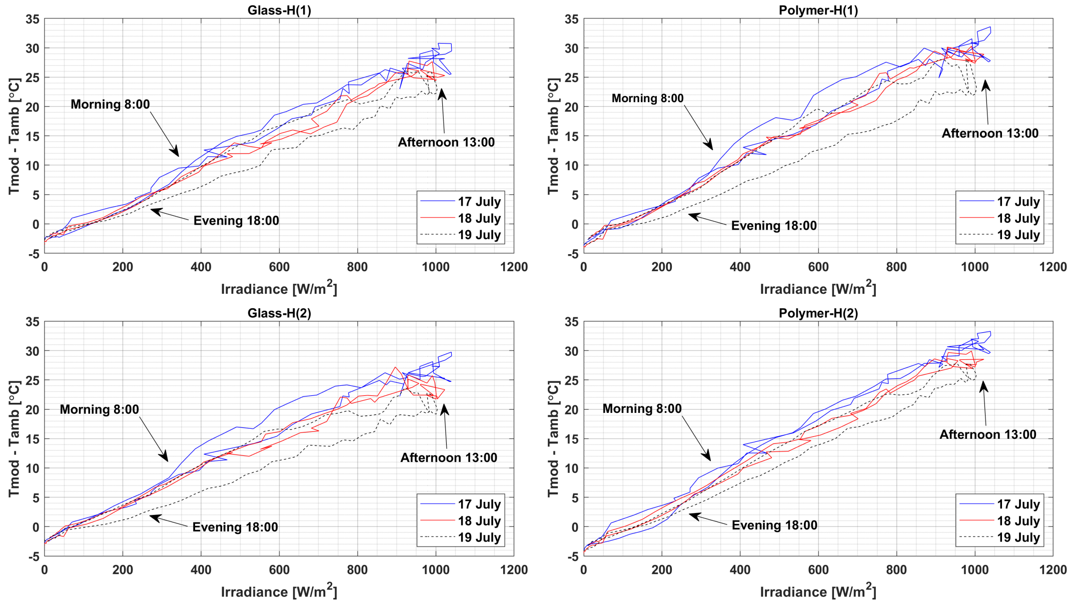

Figure 4.5: Relative cell temperature (Tmod-Tamb) response to irradiance change with top left Glass-H(1) PV module; top right Polymer-H(1) PV module; bottom left Glass-H(2) PV module; bottom right Polymer-H(2) PV module

The chosen three days have periods of overlapping irradiance and wind speeds. The temperatures, in Figure 4.5, are the average cell temperature of the module minus the ambient temperature. It can be observed from Figure 4.5 that during the time periods with similar irradiance and wind speed, the relative cell temperature of all modules show equal trends during all three days. However, it can also be observed that the increased level of irradiance during the 17th of July between 8:00 and 13:00 significantly increase the relative cell temperature for all PV modules. When this behaviour is compared to the 18th and 19th of July, it can be concluded that an increased level of irradiance results in an increased relative cell temperature. As previously mentioned, during the afternoon on the 19th of July, which is after the irradiance peak around $1000 W/m^2$, the wind speed starts increasing. This results from that point onwards a significant decrease in relative cell temperature, while the level of irradiance is comparable and the ambient temperature is much higher. This proves the cooling effect of an increased wind speed on the cell temperature of PV modules.

How does wind speed affect the cell temperature?

It was observed that an increased wind speed affects the cell temperature compared to lower wind speeds. Nevertheless, the cooling behaviour was only shown on three specific days. Therefore, wind speed affecting the cell temperature has to be analysed over a longer period. Since the polymer- and glass module are made of different materials, wind speed can affect the cell temperatures in a different order of size. The difference will therefore be measured by finding the cooling rates. All data points over the period 1 June till 30 September are collected and ordered in irradiance ranges. Reason is that the irradiance affects the cell temperature, so the creation of irradiance bins cause that the irradiance affects of the data points in the bin is similar, but that the affect of wind can be seen. All data points of the bin are then plotted with the relative cell temperature ($T_{mod} - T_{amb}$) on the y-axis and wind speed at the measured moment at the x-axis. The line, fitted thru the data points, creates the formula that presents the relative cell temperature for a given wind speed in the specific range of irradiance. The formula is described as follow:

$$T_{rel} = a * U + b \tag{4.4}$$

where a is the cooling rate [$^{\circ}C/(m * s^{-1})$], U is the wind speed[m/s] and b is the temperature constant at a wind speed of $0 m/s$.

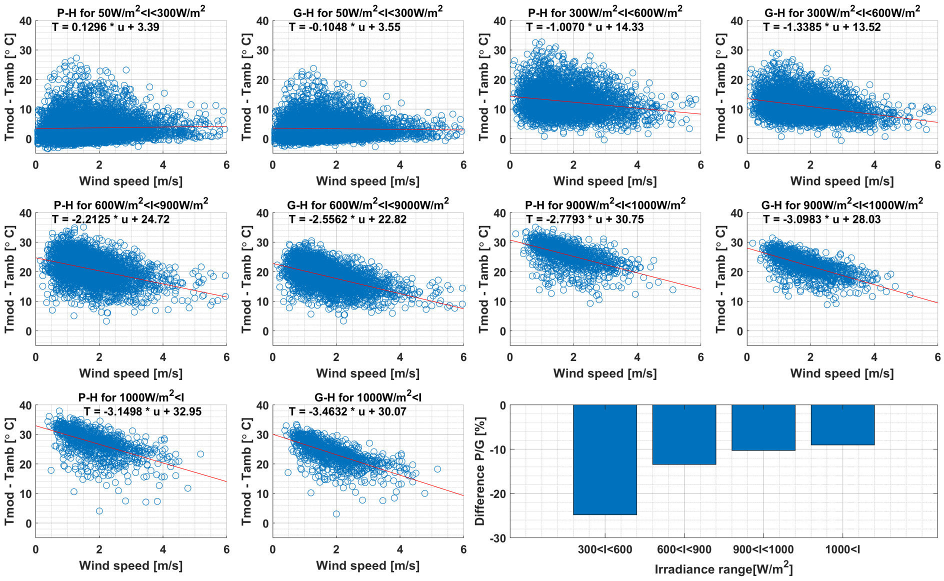

Figure 4.6: Measured relative cell temperature at measured wind speed in fixed irradiance bins. Every bin is plotted for the Polymer-H and Glass-H module is the same order. The formula in the plots corresponds with Equation 4.4; The bar plot presents the difference in cooling rate by dividing the Polymer-H cooling rate by the Glass-H cooling rate

Figure 4.6 shows that the cooling effect, by increased wind speed, increases for both modules when the level of irradiance becomes higher. However, the cooling rate is higher for the glass modules compared to the polymer modules. Resulting in a larger drop of relative cell temperature compared to the polymer modules. The difference in cooling rate, presented in Figure 4.6, shows that the difference in cooling rate between the polymer module and glass module becomes smaller when the irradiance increase.The lowest difference in cooling rate can be observed in the range of 900W/m^2 to 1000W/m^2 with a cooling rate difference of 6%. Based on the presented cooling rates, it can be concluded that glass module gets influenced most by an increased level of wind speed compared to the polymer modules.

How do changes of irradiance affect the thermal behaviour of the PV modules?

It was found that the increasing wind speed cools down the cell temperature of both the polymer- and glass modules. This was presented with data in constant irradiance bins. However, irradiance affects the cell temperature as well. Therefore the affect of irradiance on the cell temperature over the period of 1 June till 30 September will be analysed. Again, the polymer- and glass modules differ in materials and will differ in how the irradiance affects the cell temperatures. The difference will therefore be expressed in the heating rate. All data points are collected and ordered in wind speed bins. This is done to keep the affect of wind speed constant and present just the influence of the level of irradiance on the relative cell temperature. All data points of the bin are then plotted with the relative cell temperature ($T_{mod} - T_{amb}$) on the y-axis and irradiance at the measured moment at the x-axis. The line, fitted thru the data points, creates the formula that presents the relative cell temperature for a given level of irradiance in the specific wind speed range. The formula is described as follow:

$$T_{rel} = c * G + d \tag{4.5}$$

where c is the heating rate [$^{\circ}C/(Wm^{-2})$], G is the level of irradiance [W/m^2] and d is the temperature constant at a level of irradiance of $0W/m^2$.

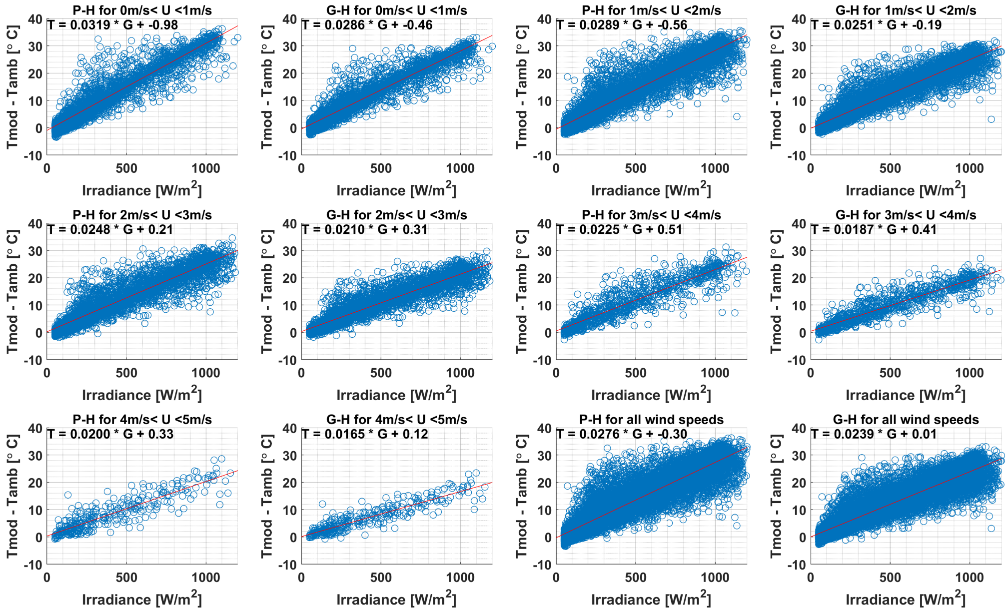

Figure 4.7: Measured average relative cell temperature at measured level of irradiance in fixed wind speed bins. Every bin is plotted for the Polymer-H and Glass-H PV modules is the same order. The formula in the plots corresponds with Equation 4.5

The correlation between the level of irradiance and relative cell temperature, presented in Figure 4.7, shows that an increasing level of irradiance will increase the cell temperature. This can be expressed in the heating rate, shown in the figure. It can be observed that the rate of heating is larger for the polymer modules compared to the glass modules. The lower the wind speed range, the larger the heating rate is for both modules. However, the pattern of irradiance during the day always shows an increase of irradiance followed by a decrease towards the end of the day. Therefore one can interpret the heating rate in two directions. It can therefore be concluded that the cell temperature of the polymer PV modules will increase faster when the level of irradiance increase, but will also cool down faster as soon as the level of irradiance decrease.

4.2.2. Electrical performance

The thermal behaviour of the PV modules are shown and the factors that influence the cell temperature are shown. It is proven that the cell temperature of the polymer PV modules are higher compared to the glass modules. Based on the theory of section 2.2 this would mean that the modules made by Solarge should have even greater maximum power point reduction compared to glass modules. Therefore, the electrical outdoor performance will be analysed and used to calculate the performance ratio and energy yield. Based on these results conclusions can be taken on the significance of temperature on the performance.

What is the energy yield of the modules?

The energy yield is calculated with Equation 2.5 and stc module power, Table 3.3, that was obtained by I-V measurements at Solarge, before the installation. The power that is used in Equation 2.5 is the measured power with the cable power loss added. The values obtained by the calculation gives the first indication of the performance comparison between modules made by Solarge and glass modules. The energy yield gives just an electrical performance, meaning that the irradiance, in contrast to the performance ratio, does play a significant role in the performance of a module. The calculations, made with the measured data were the daily energy yield calculations during the period of 1 June till 30 September. The calculated daily values were separately analysed, but also summed to get an understanding of the total energy yield difference between Polymer-H PV modules and Glass-H PV modules.

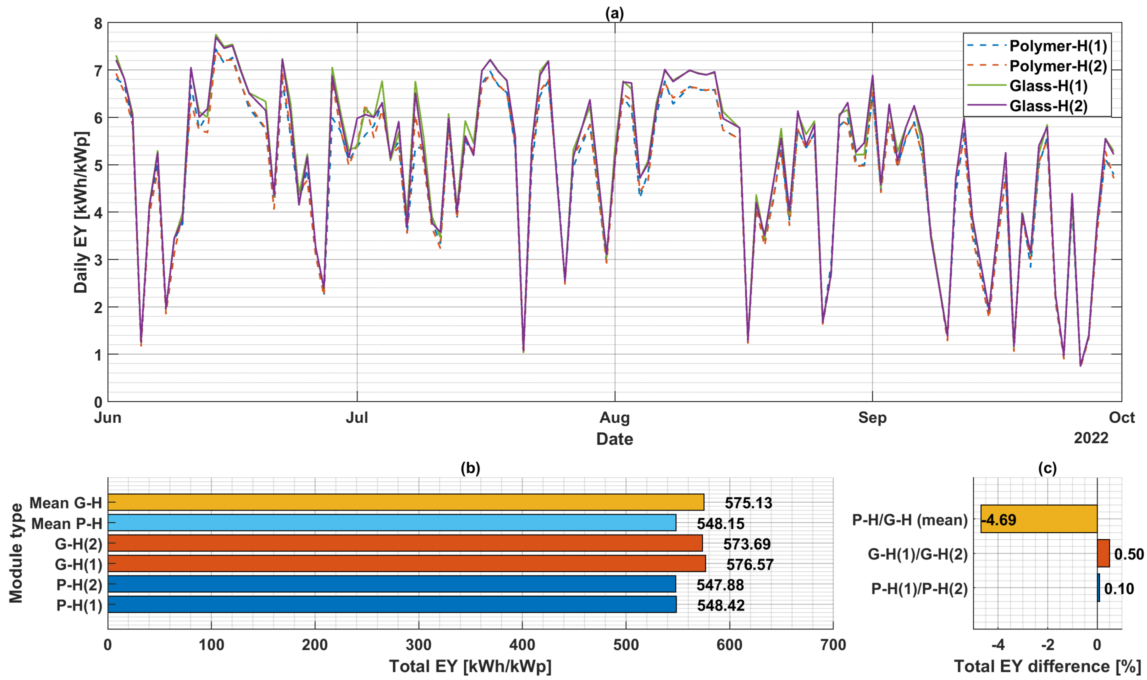

Figure 4.8: (a) Daily energy yield of the separate Polymer-H and Glass-H PV modules from 1 June till 30 September; (b) The total energy yield of the separate Polymer-H and Glass-H PV modules and the mean of Polymer-H and Glass-H PV modules from 1 June till 30 September; (c) The measured difference in total energy yield between the Polymer-H PV modules, Glass-H PV modules and the mean Polymer-H and mean Glass-H PV modules

Figure 4.8 presents the energy yield in the period between 1 June and 30 September. During days with a lot of irradiance, one can observe a large difference between polymer PV modules, made by Solarge, and glass PV modules. The difference during some days can rise up to 0.4 kWh/kWp. The average total energy yield over the entire measurement period for polymer PV modules is 548.15 kWh/kWp, while this is 575.13 kWh/kWp for the installed glass modules. This means that the modules made by Solarge have an energy yield that is 4.69% less compared to glass modules. Based on the obtained results we can conclude that the energy yield

What is the daily performance ratio over the entire measurement period?
The performance ratio is calculated with Equation 2.6 and stc module power, Table 3.3. It normalises the energy yield based on the irradiance yield. Similar to the energy yield calculation, the power that is used is the measured power with the cable power loss added. The following figure makes use of a box plot. More information about box plot theory can be found in section B.1.

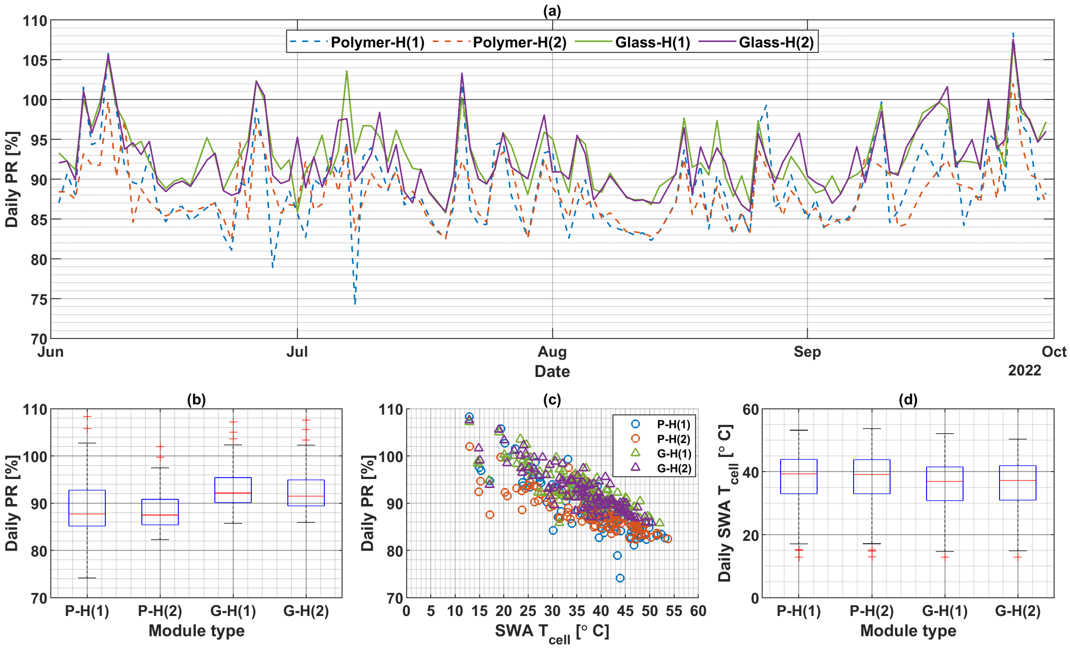

Figure 4.9: (a) Daily performance ratio of separate Polymer-H and Glass-H PV modules from 1 June till 30 September; (b) Boxplot presenting the median daily performance ratio of separate Polymer-H and Glass-H PV modules over the period of 1 June till 30 September; (c) Daily performance ratio of separate Polymer-H and Glass-H PV modules plotted against the measured SWA cell temperature of the measurement day, in the period from 1 June till 30 September;(b) Boxplot presenting the median SWA cell temperature of separate Polymer-H and Glass-H PV modules over the period of 1 June till 30 September

Figure 4.9 presents the daily performance ratio in the period between 1 June and 30 September. When the performance ratio and the energy yield are compared, one can observe that the peaks of the energy yield changed into valleys in the performance ratio. However, the performance ratio during most of the days is higher for the glass modules compared to the polymer modules. Another observation that can be made is the effect of cell temperature on the PR. It can be seen that the higher cell temperatures result in lower PR. The trend show almost the same behaviour for the polymer and glass modules, but deviates in a lower PR and the polymer modules have more days with higher SWA cell temperature compared to glass.

The box plot in Figure 4.9 presents the statistical values over the period of 1June till 30 September. More details about the box plot theory can be found in section B.1. The box plots present a lower median value for the performance ratio of polymer modules compared to the glass modules. The median values of the modules are:

- **Polymer-H(1):** PR= 87.7% SWA T_{cell}= 39.3°C
- **Polymer-H(1):** PR= 87.5% SWA T_{cell}= 39.1°C
- **Glass-H(1):** PR= 92.2% SWA T_{cell}= 36.9°C
- **Glass-H(1):** PR= 91.5% SWA T_{cell}= 37.2°C

The median PR difference between polymer modules and glass modules comes down to 3.8 - 4.7%. It can also be observed that the box and whiskers of Polymer-H(1), are much larger compared to the other modules. This can be translated in a much larger deviation of PR over the period. The median of the SWA cell temperatures proves the cell temperature difference over the entire period between Polymer-H and Glass-H modules of 1.9 to 2.4°C. The PR values that are presented are daily values, which give an understanding of the daily behaviour over a longer period and makes it easier to compare between the different modules. However, the daily PR does not explain whether the PR of the polymer based modules are the entire day below the PR of glass modules or if this behaviour just happens during a certain period of the day. Therefore the behaviour during stable irradiance days with clear sky conditions need to be compared, to see where the deviation in PR is made. The reasoning for stable irradiance days is related to the fact that clear sky conditions with stable irradiance leads to a stable generation of power. The more stable the generation is, the more stable the PR, current and voltage will be during a day plot. Stability can be translated as low fluctuation or noise withing the trend. The days that are chosen, are similar to the three days presented in Figure 4.4, namely 17 till 19 July. These days are characterised by there stable irradiance and different ambient temperatures.

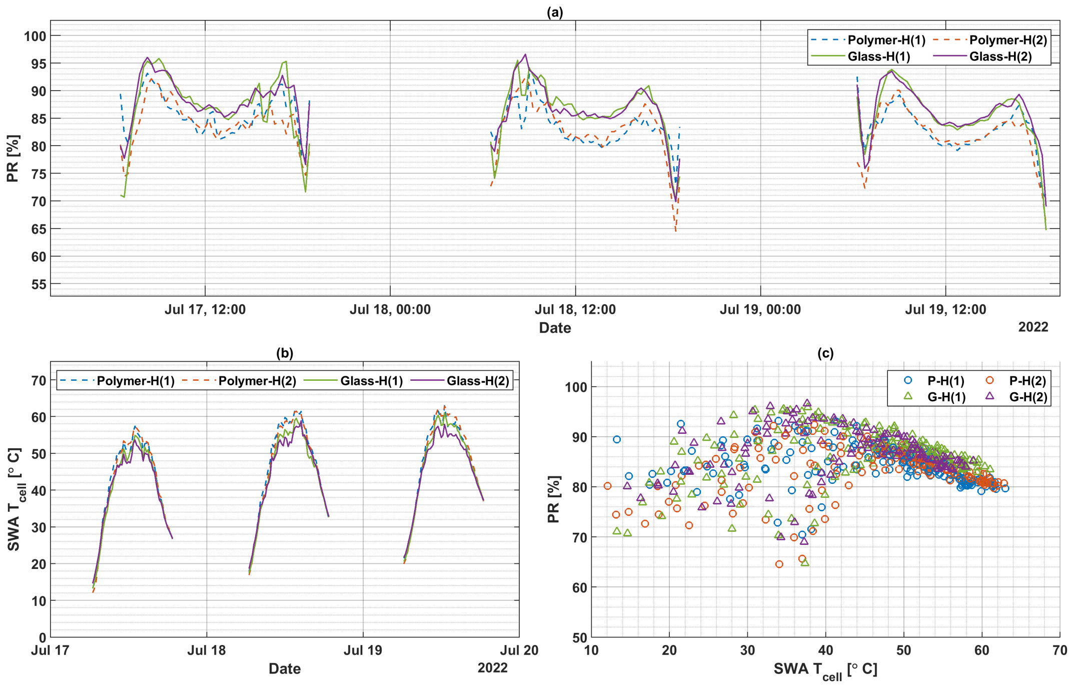

Figure 4.10: (a) Performance ratio per 15 minutes of separate Polymer-H and Glass-H PV modules on 17, 18 and 19 July;(b) SWA cell temperature per 15 minutes of separate Polymer-H and Glass-H PV modules on 17, 18 and 19 July;(c) Performance ratio per 15 minutes of separate Polymer-H and Glass-H PV modules plotted against the measured SWA cell temperature per 15 minutes of the measurement day, in the period from 17, 18 and 19 July

Figure 4.10 presents the performance ratio over 15 minutes during the days, when the irradiance is at least 50 W/m^2. It can be observed that the modules start and end the day with overlapping PR as well as SWA cell temperatures. However, between the daily peaks around 08:30 and 17:00, a deviation in performance between the polymer- and glass modules can be observed. The same behaviour can be seen from the SWA cell temperatures that are higher for the polymer modules. The half-cut cells used in the polymer- and glass modules are exactly the same, meaning that the temperature coefficient for P_{mpp}(-0.390%/$°C$), V_{oc} and I_{sc} are also the same. This taken into account, makes a cell temperature difference, between polymer- and glass module, of 5°C responsible for -1.95% lower polymer P_{mpp} compared to glass P_{mpp}. This takes place at July the 18th at 12:30. Nevertheless, the higher cell temperatures cannot be the only reason for the decrease in PR and total difference between the polymer- and glass modules. The PR shows the performance behaviour with losses in temperature, optics, electronics and uncertainties combined. However, temperature- and optical effects can best be seen when voltage and current are separtely observed. The voltage behaviour of a module will display the thermal behaviour of the module during the day, so when sufficient irradiance is available to generate electricity in the PV module.The current behaviour of a module will display the optical behaviour of the module during the day. Current is therefore strongly dependent on the level of irradiance. Other optical aspects that influence the current are the reflectance and transmittance of the front- and backsheet, but also soiling and the angle-of-incidence.

Module name	Datasheet V_{mpp} $[V]$	I-V Measurement V_{mpp} $[V]$	Δ V $[V]$	Datasheet I_{mpp} $[A]$	I-V Measurement I_{mpp} $[A]$	Δ I $[A]$
P-H(1)	35.24	34.1	-1.14	12.77*	11.85	-0.92
P-H(2)	35.24	34.1	-1.14	12.77*	11.87	-0.90
G-H(1)	31.72	30.6	-1.12	12.77	12.61	-0.16
G-H(2)	31.72	30.7	-1.11	12.77	12.67	-0.10

*Would be the same value as glass module in case of glass frontsheet

Table 4.3: Datasheet and I-V measurement I_{mpp} and V_{mpp} compared

In Table 4.3, the I-V measured V_{mpp} and I_{mpp} are compared to the values of the manufacturer data sheet. The glass- and polymer modules make use of the exact same type of PV cells, but the glass module contains 108 cells and the polymer module 120 cells. Therefore, the datasheet values for the polymer modules are calculated based on the datasheet values of the glass modules. The datsheet I_{mpp} of the polymer modules should be the exact same when the frontsheet of the polymer modules would be glass. However, the difference between the datsheet I_{mpp} and I-V measured I_{mpp} proof that during STC, with optimal irradiance and AOI, an optical loss is measured of 0.92A, or -7.2%. This loss can most certain be related to the polymer frontsheet. The outdoor measurement setup also collects the V_{mpp} and I_{mpp} data of the modules. Therefore, the current, voltage and power are normalised with the I-V measured mpp values, to be able to compare the modules.

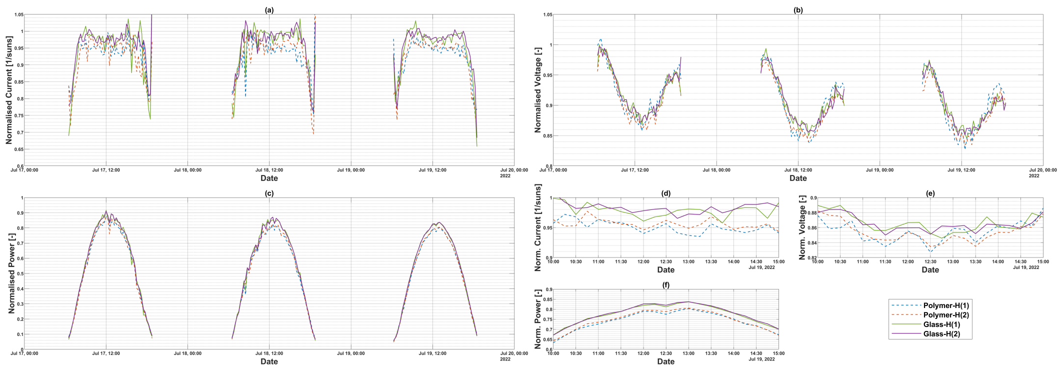

Figure 4.11: (a) Normalised current expressed per sun with data points per 15 minutes of separate Polymer-H and Glass-H PV modules on 17, 18 and 19 July;(b) Normalised voltage with data points per 15 minutes of separate Polymer-H and Glass-H PV modules on 17, 18 and 19 July;(c) Normalised power with data points per 15 minutes of separate Polymer-H and Glass-H PV modules on 17, 18 and 19 July; (d) Normalised current expressed per sun with data points per 15 minutes of separate Polymer-H and Glass-H PV modules zoomed on the 19th of July;(e) Normalised voltage with data points per 15 minutes of separate Polymer-H and Glass-H PV modules zoomed on the 19th of July;(f) Normalised power with data points per 15 minutes of separate Polymer-H and Glass-H PV modules zoomed on the 19th of July;

Again the performance of the modules are compared during the 17th till 19th of July. Since these days have stable irradiance levels, this can show more stable behaviour and expose losses in a clearer way. Figure 4.11 shows that the normalised power is larger for the glass modules compared to the polymer modules. Then, by looking at the current an voltage behaviour, the optical and thermal behaviour is being exposed. First, the voltage level for all modules show clear response to the increasing cell temperature during the day. Also, the larger reduction of voltage compared to the smaller increase in current by temperature makes that the cells show a reduced power output by increasing temperatures. Therefore, small differences in normalised voltage levels between the polymer- and glass modules will impact the power difference. However, the zoomed normalised voltage level during the 19th of July, shows that the voltage behaviour of the polymer- and glass modules are more or less similar. There is no clear difference between the modules, eventhough the cell temperatures are higher for the polymer modules, as can be seen in Figure 4.10. Second, the current level for all modules show clear response to the increasing level of irradiance during the day. However, compared to the volatge level, it can now be clearly seen that the current level is lower for the polymer modules compared to the glass modules. This proofs that the polymer modules show a significant current difference, which origins most certainly from optical losses.

4.2.3. Conclusions

All analysis, calculations and results are presented for the polymer-H and glass-H modules. First the thermal behaviour of the modules were presented. It was found that the wind speed affects the cell temperature of glass modules most. The smallest difference in cooling rate, between polymer- and glass modules, was found for a level of irradiance above 1000 W/m^2. The level of irradiance affects the polymer modules most. The cell temperatures rise faster for the polymer modules compared to the glass modules. Overall, the SWA cell temperature of the modules, from 1June till 30 September, was higher for the polymer modules, [39.1 - 39.3]$°C$, compared to the glass modules, [36.9 - 37.2]$°C$.

On the electrical behaviour it was found that the glass modules produced the highest energy yield compared to the polymer modules. Over a period of 1 June till 30 September it was found to -4.69% less for polymer modules. Looking further to the daily PR, it was seen that the glass modules had a higher daily PR, [91.5 - 92.2]%, compared to the polymer modules, [87.5 - 87.7]%. When the normalised current and voltage were presented for 17 till 19 July, it was seen that the normalised current as well as the normalised voltage showed a lower values compared to the glass modules. Based on the SWA cell temperatures that were higher for the polymer modules, it was expected to result in lower performance values for the polymer modules compared to the glass modules. However, the relative small differences presented in the normalised current and voltage plots cannot make up the entire difference in performance. The origin of the small measured difference can come form the measurement uncertainties, resistance losses or other, yet, unknown causes.

4.3. Outdoor performance of polymer-F-White and -Black backsheet modules

In section 4.2 the thermal behaviour and electrical performance of the polymer- and glass modules were discussed with results of the outdoor measurement setup. The outdoor measurement setup also contains white- and black polymer modules of which the thermal- and electrical data are collected. The performance results of both white- and black polymer modules will be discussed in the same order, as done for the polymer with glass comparison. First, the results of the thermal behaviour of the modules will be shown, followed by the electrical performance. The data, used to analyse, covers the time period between 1 June and 30 September 2022.

4.3.1. Thermal behaviour results

In subsection 4.2.1 it was said that the the thermal behaviour of a PV module can best be explained by measuring the cell temperature of the module. Therefore, the the polymer-white and polymer-black modules also contain temperature sensors in the backsheet. In this way, the influence of backsheet color on the cell temperature and therefore the electrical performance can be researched. Before further analysis were made, the temperature sensor data was checked and compared with sensors on the same module. The data showed a much lower temperature for the right side located sensor on the polymer-black(1) module (Polymer-F-B(1)), while all other modules showed that the left sensor was lower. Therefore the right sensor of BB1 was taken out of further analysis.

What cell temperatures do the modules have?

The first understanding of the module behaviour is made by looking closer to the cell temperatures at specific days. Since the polymer-F-white and polymer-F-black modules are installed on the exact same roof as the polymer-H and glass-H modules, the same specific days are used from Table 4.1, in subsection 4.2.1. The chosen days are based on a clear- or cloudy sky and high or low ambient temperatures.

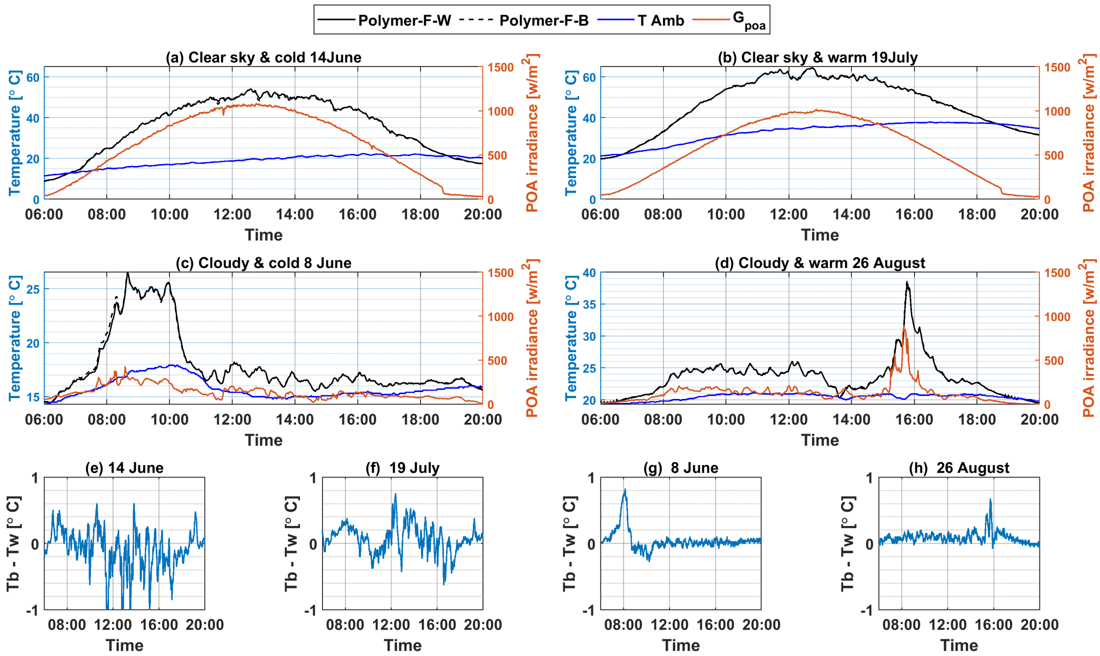

Figure 4.12: Measured Polymer-F-White and Polymer-F-Black PV module cell temperatures, ambient temperature and general plane-of-array irradiane at (a) clear sky & low ambient temperature 14 June; (b) clear sky & high ambient temperature 19 July; (c) cloudy sky & low ambient temperature 8 June; (d) cloudy sky & high ambient temperature 26 August; The measured cel temperature difference between Polymer-F-White and Polymer-F-Black on (e) 14 June; (f) 19 July; (g) 8 June; (h) 26 August

The module temperatures, shown in Figure 4.12, are the average module temperature. It can be observed that cell temperatures of the polymer-F-white and polymer-F-black follow the same pattern and are overlapping most of the time. The plots in the bottom of Figure 4.12, confirm the visual observation. The cell temperature difference between the polymer-F-white and polymer-F-black fluctuates around the $0°C$ with a maximum difference of $\pm\ 1°C$. Based on the shown figure, no clear difference in cell temperature can be observed. Where during clear sky conditions, the cell temperature of the polymer-H and glass-H showed a clear increase in cell temperature and difference related to irradiance, this can not be observed for the polymer-F-white and polymer-F-black modules.

Date	T_{Amb} [$°C$]	P-F-W(1) [$°C$]	P-F-W(2) [$°C$]	P-F-W [$°C$]	P-F-B(1) [$°C$]	P-F-B(2) [$°C$]	P-F-B [$°C$]	W-B [$°C$]
14 June	19.0	43.9	43.2	43.5	42.3	44.4	43.4	0.2
19 July	34.0	54.6	53.7	54.1	53.3	55.1	54.2	-0.1
8 June	16.1	19.3	19.3	19.3	19.3	19.4	19.3	-0.1
26 August	20.5	25.3	26.3	25.8	26.1	25.7	25.9	-0.2

Table 4.4: Solar weighted cell temperatures on the specific days for the polymer-F-white and -black modules

Table 4.4 expresses the solar weighted average (SWA) cell temperatures of the modules during the specifically chosen days. Again, the SWA cell temperatures show a minimal temperature difference over the day. Nevertheless, the results that are shown, are just four days of the entire measurement period from 1 June till 30 September. Therefore, the marginal cell temperature difference that is observed during these four days could always be the behaviour, but can also be an exception. The influence of wind is one of the factors that could influence the cell temperature difference. Table 4.1 shows that the average wind speed during the 19th of July was around $1m/s$ higher compared to the 14th of June. The influence of different wind speeds on the cell temperature of the PV modules will therefore be analysed in more detail. The influence of wind speed is shown, based on 3 days in a row that show stable irradiance, while having varying wind speeds. The chosen days are 17, 18 and 19 July and visualised in Figure 4.4. The ambient temperatures differ much between the days, while the irradiance is overall the same, with the exception of the 17th of July between 9:30 and 12:00. The wind speed differs most on the 19th of July during the afternoon with 1 to 2m/s wind speed difference compared to the 17th and 18th of July.

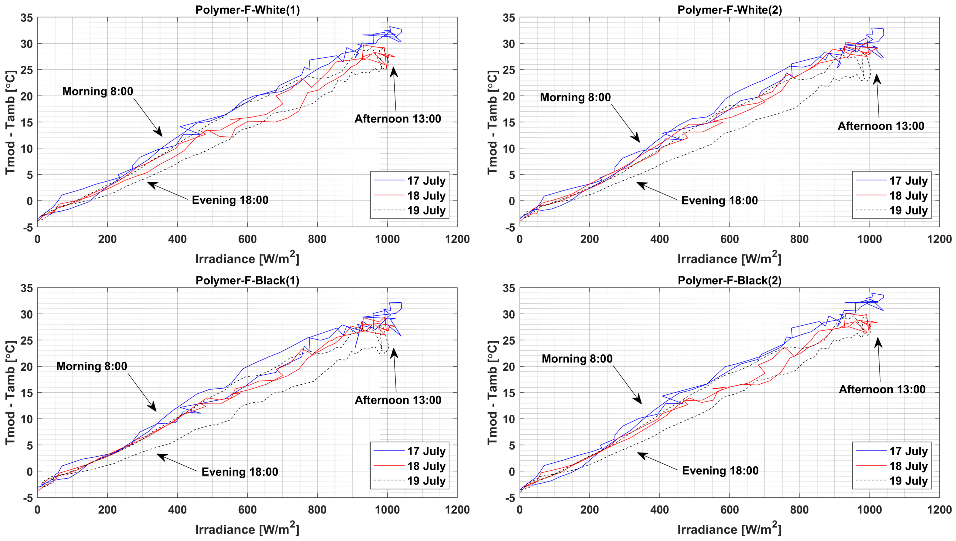

Figure 4.13: Relative cell temperature (Tmod-Tamb) response to irradiance change with top left Polymer-F-White(1) PV module; top right Polymer-F-White(2) PV module; bottom left Polymer-F-Black(1) PV module; bottom right Polymer-F-Black(2) PV module

It can be observed, from Figure 4.13, that during periods with similar wind speed, which is the case during from 17 till around 12:30 at 19 July, the relative cell temperatures of the modules are similar. However, the effect of increased wind speed at the 19th of July at noon becomes visible in the figure. Polymer-F-White(2) and Polymer-F-Black(1) show a lower relative cell temperatures compared to the other days and modules. This proves that wind does have an effect on the cell temperatures of the Polymer-F-White and Polymer-F-Black modules. Furthermore, Polymer-F-White(2) and Polymer-F-Black(1) are both positioned on the right side of the roof. The right side of the roof is oriented to the east. The increased wind speed at the 19th of July comes from the east, which explains the larger effect of wind on the cell temperature of Polymer-F-White(2) and Polymer-F-Black(1), compared to the other two modules.

What is the cell temperature response to different wind speeds?

After proving the effect of wind speed on the cell temperature of the Polymer-F-White and Polymer-F-Black modules, an in-dept analysis can be made on the effect of varying wind speed during a fixed irradiance range.

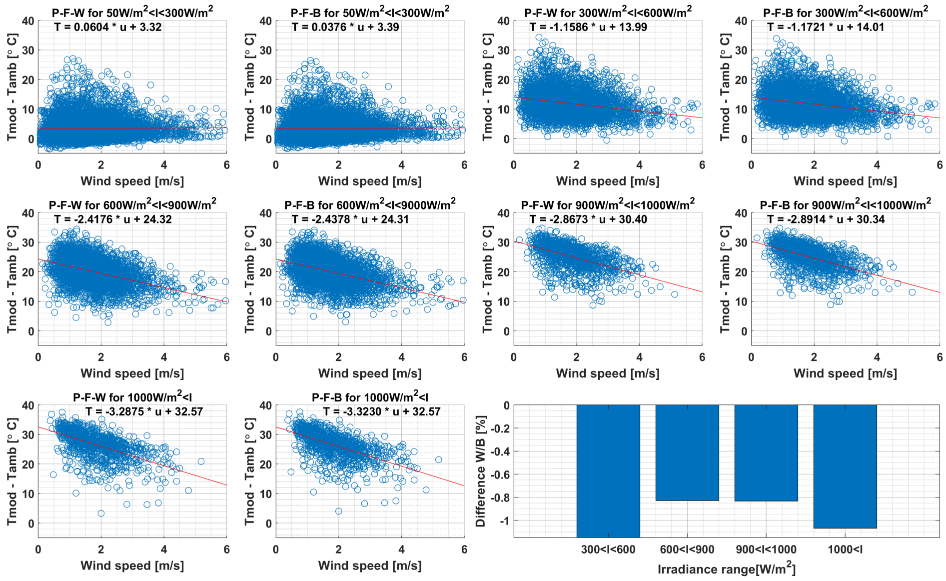

Figure 4.14: Measured relative cell temperature at measured wind speed in fixed irradiance bins. Every bin is plotted for the polymer- and glass module is the same order. The formula in the plots corresponds with Equation 4.4; The bar plot presents the difference in cooling rate by dividing the Polymer-F-White cooling rate by the Polymer-F-Black cooling rate

The results, shown in Figure 4.15, present lower relative cell temperatures with increasing wind speeds for irradiance levels above 300W/m^2. The higher the level off irradiance, the higher the cell temperature will be. This also result in a larger cooling rate dependent on wind speed level. When the Polymer-F-White and Polymer-F-Black modules are compared, it can be observed that the maximum difference in cooling rate occurs in the range of 300W/m^2 to 600W/m^2. The maximum difference is -1.15% when the Polymer-F-White is compared to Polymer-F-Black. The bargraph shows that in all ranges the cooling rate of the Polymer-F-White is lower compared to Polymer-F-Black, meaning that the PV cells in the polymer modules with a black backsheet will cool faster by the influence of wind speed compared to the PV cells in the polymer modules with a white backsheet. However, the difference in cooling rate is marginal and can therefore be considered as comparable cooling rates. This can be substantiated with a quick calculation for the irradiance range of 1000W/m^2 and above. When a wind speed of 4m/s is taken, the cell temperature of Polymer-F-White modules will decrease with 13.15$°C$ while the cell temperature of Polymer-F-Black will decrease with 13.29$°C$. This comes down to a difference in cell temperature reduction of 0.14$°C$, which is negligible. The fact that the cooling rate is comparable also proves that the material and layer thickness are identical. The black color does not effect the cell temperature when compared to wind speed. Therefore, the influence of the level of irradiance and the cell temperature response will be further analysed.

What is the cell temperature response on irradiance change?

The effect of wind speed on the cell temperature of the Polymer-F-White and Polymer-F-Black modules are presented and show similar cooling rates. The following and most important influence on the cell temperature is irradiance. In Figure 4.12 it was observed that the higher level of irradiance results in higher cell temperatures. The influence of irradiance under stable wind speed will therefore be further analysed.

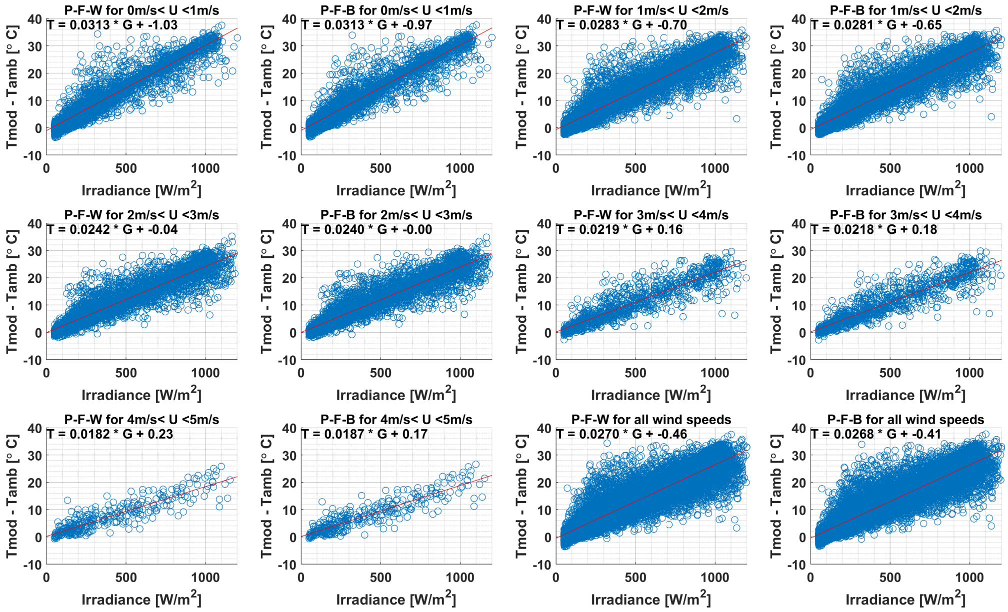

Figure 4.15: Measured average relative cell temperature at measured level of irradiance in fixed wind speed bins. Every bin is plotted for the Polymer-F-White and Polymer-F-Black PV modules is the same order. The formula in the plots corresponds with Equation 4.5

Figure 4.15 presents the influence of varying irradiance in consistent ranges of wind speed. It can be observed from all wind speed ranges that the heating rate of irradiance is similar for both Polymer-F-White and Polymer-F-Black modules. The heating rate for all wind speeds is 0.0270 $^{\circ}C/(Wm^{-2})$ for Polymer-F-White modules and 0.0268 $^{\circ}C/(Wm^{-2})$ for Polymer-F-Black modules. Using a quick calculation, this means that at 1000 W/m^2) the Polymer-F-White modules heated 27.0$^{\circ}C$, while Polymer-F-Black modules heated 26.8$^{\circ}C$. This is a small difference of 0.2$^{\circ}C$ and therefore negligible considering the cell temperatures. This proves that the black backsheet color of the polymer module does not heat the PV cells faster compared to the white backsheet color of the polymer module.

4.3.2. Electrical performance

The results considering thermal behaviour of the modules, influenced by irradiance and wind speed, are presented and no clear temperature difference was seen. That does not mean that the electrical performance of the modules are similar as well. Therefore, the electrical performance of the Polymer-F-White and Polymer-F-Black modules will be analysed and compared in this section.

What is the energy yield of the modules?

The energy yield is calculated with Equation 2.5 and stc module power, Table 3.3, that was obtained by I-V measurements at Solarge, before the installation. The power that is used in Equation 2.5 is the measured power with the cable power loss added. The values obtained by the calculation gives the first indication of the performance comparison between the Polymer-F-White and Polymer-F-Black modules. The energy yield gives just an electrical performance, meaning that the irradiance, in contrast to the performance ratio, does play a significant role in the performance of a module.

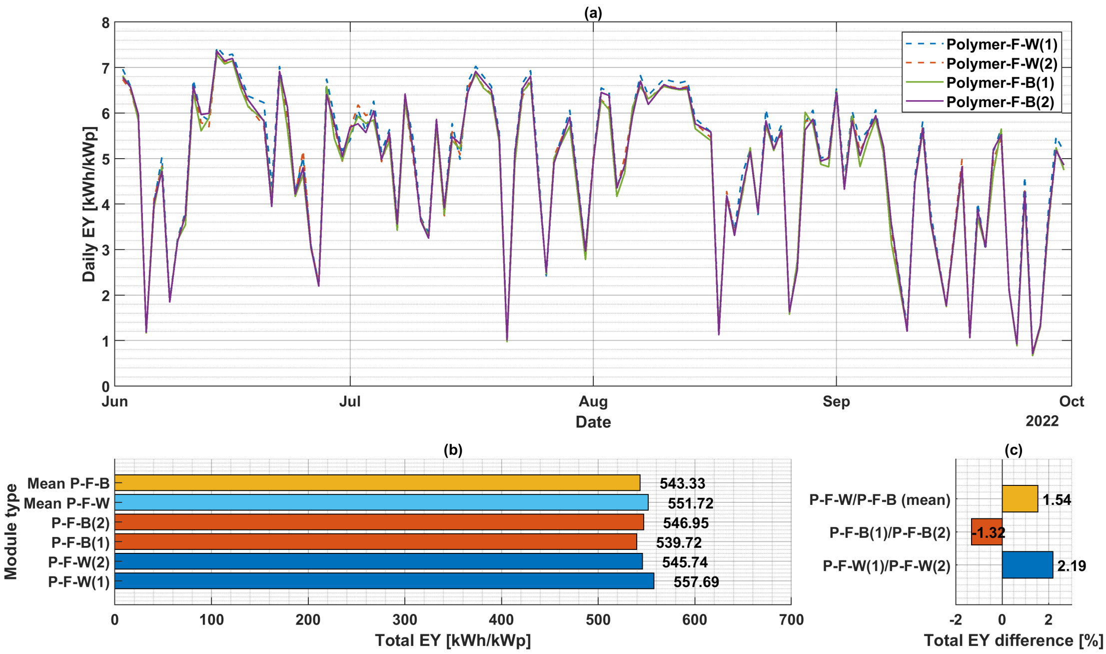

Figure 4.16: (a) Daily energy yield of the separate Polymer-F-White and Polymer-F-Black PV modules from 1 June till 30 September; (b) The total energy yield of the separate Polymer-F-White and Polymer-F-Black PV modules and the mean of Polymer-F-White and Polymer-F-Black PV modules from 1 June till 30 September; (c) The measured difference in total energy yield between the Polymer-F-White PVmodules, Polymer-F-Black PV modules and the mean Polymer-F-White and mean Polymer-F-Black PV modules

Figure 4.16 presents the energy yield in the period between 1 June and 30 September. During days with high level of irradiance, one can observe the same EY peaks during these days. However, the blue dotted line of the Polymer-F-White(1) module is most often performing at a higher EY compared to the other modules, while Polymer-F-Black(1) is most often performing at a lower EY. The difference during some days can rise up to 0.4 kWh/kWp between the Polymer-F-White(1) and Polymer-F-Black(1) module. The difference between the named modules can also be seen in the total energy yield during the period between 1 June and 30 September.The average total energy yield over the entire measurement period for Polymer-F-White modules is 551.72 kWh/kWp, while this is 543.33 kWh/kWp for the installed Polymer-F-Black modules. When this is translated into percentages, Polymer-F-White modules measured a 1.54% higher EY compared to Polymer-F-Black modules. Based on the obtained results we can conclude that the Polymer-F-White modules produced on average more energy compared to Polymer-F-Black modules. However, on individual module level, it can be observed that the EY of Polymer-F-White(2) was slightly lower compared to Polymer-F-Black(2). Only based on the EY, this could mean that the black backsheet modules produce indeed less energy compared to the white backsheet modules or that the position on the roof, measurement uncertainties or damages in the black backsheet modules created the difference. Therefore, further analysis will be done with the performance ratio.

What is the daily performance ratio over the entire measurement period?

The energy yield of the Polymer-F-White and Polymer-F-Black modules are analysed, presented and showed a difference in energy yield. The performance ratio will show the performance where the direct influence of irradiance is normalised, leaving the influence of temperature, uncertainties and losses left. The performance ratio is calculated with Equation 2.6 and stc module power, Table 3.3. Similar to the energy yield calculation, the power that is used is the measured power with the cable power loss added. The following figure makes use of a box plot. More information about box plot theory can be found in section B.1.

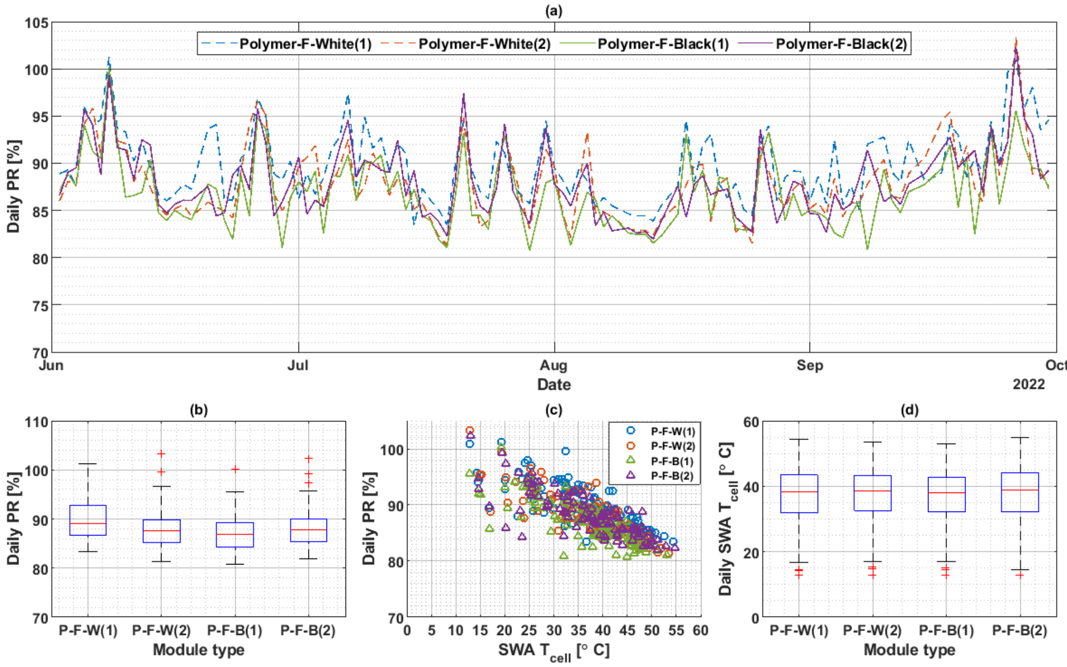

Figure 4.17: (a) Daily performance ratio of separate Polymer-F-White and Polymer-F-Black PV modules from 1 June till 30 September; (b) Boxplot presenting the median daily performance ratio of separate Polymer-F-White and Polymer-F-Black PV modules over the period of 1 June till 30 September; (c) Daily performance ratio of separate Polymer-F-White and Polymer-F-Black PV modules plotted against the measured SWA cell temperature of the measurement day, in the period from 1 June till 30 September;(b) Boxplot presenting the median SWA cell temperature of separate Polymer-F-White and Polymer-F-Black PV modules over the period of 1 June till 30 September

Figure 4.17 presents the daily performance ratio of the Polymer-F-White and Polymer-F-Black modules over a period from 1 June till 30 September. It can be observed that again the Polymer-F-White(1) and Polymer-F-Black(1) modules are the high and low performing modules. It can be clearly seen that the during almost all days, the Polymer-F-White(1) has a higher performance compared to the other modules. The visual observation is confirmed by the boxplot in the same Figure 4.17. The median values for the daily PR and daily SWA cell temperature of the modules are:

- **Polymer-F-White(1):** PR=89.1% SWA T_{cell}= 38.3$°C$
- **Polymer-F-White(2):** PR=87.7% SWA T_{cell}= 38.7$°C$
- **Polymer-F-Black(1):** PR=86.8% SWA T_{cell}= 38.1$°C$
- **Polymer-F-Black(2):** PR=87.8% SWA T_{cell}= 38.7$°C$

The median daily PR difference between polymer-F-White modules and Polymer-F-Black modules is maximum 2.3% and minimum is -0.1%, meaning the black backsheet module has a 0.1% higher daily PR. If the focus is mainly on the Polymer-F-White(1) modules, it can be said that the white backsheet modules clearly perform better compared to the black backsheet modules. However, Polymer-F-White(2) performed similar to the Polymer-F-Black(2) module. Also the daily PR against daily solar weighted average cell temperatures of the modules show the same trend. The median daily SWA cell temperature values also proof that the difference between the white backsheet modules and black backsheet modules is negligible.

It has been shown that the daily performance and cell temperatures are comparable for Polymer-F-White and Polymer-F-Black modules. Therefore, a closer look will be taken on the performance and thermal behaviour during a day. Because of random measured electrical data of the modules for every random 'X' number of minutes, the smallest time stamp that can be taken is 15 minutes.

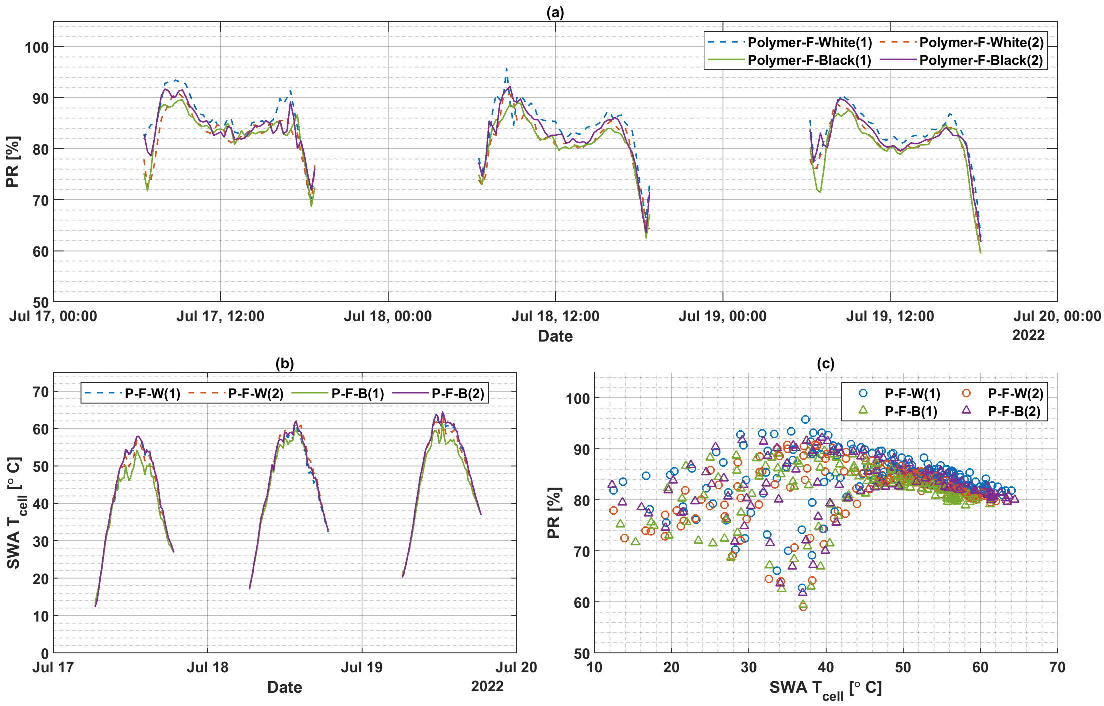

Figure 4.18: (a) Performance ratio of Polymer-F-White and Polymer-F-Black modules at 17, 18 19 July; (b) Solar weighted average cell temperature of Polymer-F-White and Polymer-F-Black modules at 17, 18 19 July; (c) Performance ratio at measured SWA cell temperature of Polymer-F-White and Polymer-F-Black modules

It can be observed fromFigure 4.18that again Polymer-F-White(1) is the module performing at a higher PR during all three days compared to the other modules, where Polymer-F-Black(1) is the under performing module. However, it is known from the literature study, that the higher cell temperatures will decrease the open-circuit voltage, decreasing the performance of the cells and therefore the module. The SWA cell temperatures show that the cell temperature of Polymer-F-Black(1) is everyday lower compared to the other modules, with outliers of around $7°C$ difference. Nevertheless, the PR of the same module proves that the lower cell temperature does result in this case to a better performance ratio. It is also good to mention again that for the Polymer-F-Black(1) module just one sensor is used, since the second sensor showed a large deviation compared to all other sensors. This can therefore be a reason that Polymer-F-Black(1) shows a much lower cell temperature. However, Polymer-F-Black(1) and Polymer-F-White(1) are both positioned on the highest point of the roof, where Polymer-F-White(1) also show a lower temperature compared to Polymer-F-White(2) and Polymer-F-Black(2). This is a sign that a lower cell temperature for Polymer-F-Black(1) can be a true measurement. The SWA cell temperatures compared with the PR did not lead to direct answers regarding the PR difference between the Polymer-F-White and Polymer-F-Black modules. This raises the question, weather the difference in EY and PR origins in the cell temperatures, optics, other losses or measurement uncertainties. Therefore, the measured power need to be split into current and voltage, to see both behaviours during the day. This will be done by normalising the measured power, current and voltage by the measured mpp values of the I-V measurement.

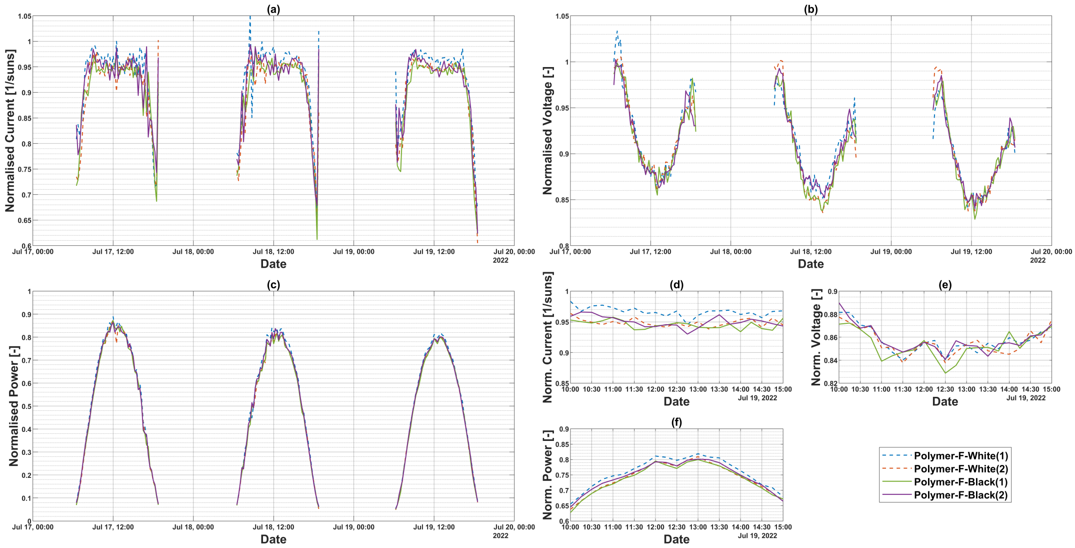

Figure 4.19: (a) Normalised current expressed per sun with data points per 15 minutes of separate Polymer-F-White and Polymer-F-Black PV modules on 17, 18 and 19 July;(b) Normalised voltage with data points per 15 minutes of separate Polymer-F-White and Polymer-F-Black PV modules on 17, 18 and 19 July;(c) Normalised power with data points per 15 minutes of separate Polymer-F-White and Polymer-F-Black PV modules on 17, 18 and 19 July; (d) Normalised current expressed per sun with data points per 15 minutes of separate Polymer-F-White and Polymer-F-Black PV modules zoomed on the 19th of July;(e) Normalised voltage with data points per 15 minutes of separate Polymer-F-White and Polymer-F-Black PV modules zoomed on the 19th of July;(f) Normalised power with data points per 15 minutes of separate Polymer-F-White and Polymer-F-Black PV modules zoomed on the 19th of July

Figure 4.19 presents the normalised values of the Polymer-F-White and Polymer-F-Black modules. It can be observed that the current values overlap most of the time, with Polymer-F-White(1) having daily a higher normalised current value between 10:00 and 15:00. The other three modules show line fluctuations that overlap and do not show a strong difference. On the other hand, the normalised voltage does show a difference in performance. The most clear day is the the 18th of July where both Polymer-F-White(2) and Polymer-F-Black(1) show a lower normalised voltage level compared to Polymer-F-White(1) and Polymer-F-Black(2). Voltage is strongly influenced by the cell temperature, so if Figure 4.18 is taken into account, it can be observed that the highest measured SWA cell temperature was the Polymer-F-White(2) module during 10:00 and 17:00. This would explain the lower voltage level for Polymer-F-White(2). However, Polymer-F-Black(1) showed the lowest SWA cell temperature during the same time period. Based on the behaviour of the normalised voltage and PR, which are both comparable to Polymer-F-White(2), and the fact that just one sensor is being used, it can be said that the SWA cell temperature of Polymer-F-Black(1) should be higher compared to what is presented in Figure 4.18. Furthermore, the 19th of July present again similar results for the modules, showing no strong deviation between the PV modules.

4.3.3. Conclusions

All analysis, calculations and results are presented for the polymer-F-White- and polymer-F-Black PV modules. First the thermal behaviour of the PV modules were presented. It was found that increasing wind speeds affects the cell temperature of the Polymer-F-Black modules most. The smallest measured difference, 1.15%, in cooling rate was found for irradiance levels between $300W/m^2 and 600W/m^2$. The level of irradiance affects the cell temperature of both the Polymer-F-White and Polymer-F-Black modules with the similar rate of 0.0270 $°C/(Wm^{-2})$ compared to 0.0268 $°C/(Wm^{-2})$. Overall, the SWA cell temperature, from 1June till 30 September, for the Polymer-F-White modules was, [38.3 - 38.7]$°C$, compared to the Polymer-F-Black modules, [38.1 - 38.7]$°C$. The hypothesis was that the modules with a black backsheet would measure higher cell temperatures since black surfaces absorb more heat than any color. Nevertheless, the SWA cell temperature was found to be comparable as well.

On the electrical behaviour it was found that the Polymer-F-White PV modules produced the highest energy yield compared to the Polymer-F-Black PV modules. Over a period of 1 June till 30 September it was found to be 1.54% higher for Polymer-F-White PV modules. Looking further to the daily PR, it was found that the Polymer-F-White modules had a higher daily PR, [87.7 - 89.1]%, compared to the Polymer-F-Black modules, [86.8 - 87.8]%. The separate analysis of MPP current and MPP voltage allowed to find optical and thermal influence on the performance of the modules. After normalising current and voltage with the indoor I-V measurement STC values, the modules were able to be compared. The figure presented a normalised current difference where just one Polymer-F-White module showed a maximum of 2% higher normalised current compared to all other modules. Since the higher normalised current was just measured for one Polymer-F-White module, the measured current of both Polymer-F-White modules could deviated because of measurement uncertainty. In case of normalised voltage the difference for all modules were negligible. The negligible difference in normalised voltage between Polymer-F-White modules and Polymer-F-Black modules is a result of the comparable cell temperatures.

5

Conclusions and Outlook

In this thesis work, polymer PV modules, made by Solarge, and glass PV modules were installed, measured and compared aiming at the understanding of the thermal- and electrical behaviour of polymer modules. In this chapter the main findings from this thesis project are summarised in the same sequence of the research objectives that were defined insection 1.4. First the main conclusions are presented section 5.1 followed by the discussion in section 5.2.

5.1. Conclusions

Before any research objectives were analysed and research questions answered, the PV modules needed for the research had to selected. The two comparison that are made to answer the objectives are polymer modules, made by Solarge, with glass modules and polymer modules containing a white backsheet with polymer modules containing a black backsheet. The modules for the polymer versus glass comparison make use of half-cut cells while the white backsheet polymer module versus black backsheet polymer module make use of full cells.

Before the selected modules were installed, pre-checks were executed to have all details of the module before the installation. The checks consisted of electroluminescence (EL) to find any cracks or dark spots and I-V measurements to characterize the performance of the PV module under standard test conditions(STC). The I-V measurements were compared with the manufacturer labels that were present on the polymer modules with a white backsheet and glass modules. The P_{STC} value of the glass modules were on average 4.44% lower compared to the manufacturer label, while the white backsheet polymer modules showed on average 3.95% lower P_{STC}. After the installation of all modules and connection of the measurement instruments, data was collected. Based on the power deviation found during the I-V measurements, it was decided to find the P_{STC} values under outdoor conditions with the collected data from the experimental setup. The goal was to further validate the P_{STC} values that were found during the I-V measurements, to allow further analysis with the data of the I-V measurements. The data was filtered based on the following parameters:

- **Irradiance:**$950W/m^2 \leq G \leq 1050W/m^2$
- **Altitude of the sun:** $\geq 55°$
- **GHI/DHI:** ≤ 0.400
- **Wind speed:** $\leq 2m/s$
- **Minimum power level:** For white- and black backsheet polymer modules$\geq 250W$. For polymer- and glass modules $\geq 275W$

After the first analysis, the P_{STC} value retrieved from the outdoor data was far lower compared to the indoor I-V measurement P_{STC} values. Resistance losses caused by the PV cables from the module to the power optimizers, was found to be the biggest loss factor. The addition of power lost in the cables resulted in outdoor P_{STC} values for the majority a deviation of lower than -5.7%, except for just one module. After the analysis of the P_{STC} values, it was decided that the measured data from the indoor I-V measurements were able to be used for further comparison analysis.

The first research objective focused on the comparison between Polymer modules with half-cut cells(Polymer-H) and glass modules with half-cut cells(Glass-H). The first comparison was made regarding the thermal behaviour of the modules. This was done by three metrics to compare the difference. Namely the cooling rate by wind speeds, heating rate by irradiance and the solar weighted (SWA) cell temperature over the period of 1 June till 30 September. First, the difference in cooling rate by the wind speed. It was found that increasing wind speeds affects the cell temperature of the Glass-H modules most. The smallest measured difference, 6%, in cooling rate was found for irradiance levels above $1000W/m^2$. Second, the heating rate by the level of irradiance. It was found that the level of irradiance affects the cell temperature of the polymer-H modules most with a heating rate of 0.0276 $°C/(Wm^{-2})$ compared to 0.0239 $°C/(Wm^{-2})$. Finally, the SWA cell temperature over the period of 1 June till 30 September was evaluated from the measured data. This was found to be higher for the polymer-H modules, [39.1 - 39.3]$°C$, compared to the glass-H modules, [36.9 - 37.2]$°C$. The second comparison was made regarding the electrical performance of the modules. First the energy yield (EY) was measured over the period of 1 June till 30 September. It was found to be -4.69% less for polymer-H modules compared to the glass-H modules. Second, the daily performance ratio (PR) was measured over the period of 1 June till 30 September. It was found that the glass modules had a higher daily PR, [91.5 - 92.2]%, compared to the polymer-H modules, [87.5 - 87.7]%. The first hypothesis was that this difference was made by the difference in measured cell temperatures. The separate analysis of MPP current and MPP voltage allowed to partly separate optical and thermal influence on the performance of the modules. After normalising current and voltage with the indoor I-V measurement STC values, the modules were able to be compared. fig. 4.11 presented a normalised current difference ranging between 0% and -4% for the polymer-H modules. This shows that the polymer-H modules likely suffer more optical losses compared to the glass-H modules. In case of normalised voltage the difference was ranging between 0% and -2% for the polymer-H modules. The reduced normalised voltage for the polymer-H modules is a result of the higher cell temperatures compared to the glass-H modules. It can be concluded that polymer-H modules face higher cell temperatures that reduce the power output of the modules. However, the normalised current showed that optical losses also contribute to the reduced power output of the polymer-H modules.

The second research objective focused on the comparison between white backsheet polymer modules with full cells (Polymer-F-White) and black backsheet polymer modules with full cells (Polymer-F-Black). The first comparison was made regarding the thermal behaviour of the modules. The same metrics used in the previous analysis were considered over the period of 1 June till 30 September. First, the difference in cooling rate by the wind speed. It was found that increasing wind speeds affects the cell temperature of the Polymer-F-Black modules most. The smallest measured difference, 1.15%, in cooling rate was found for irradiance levels between $300W/m^2$ and $600W/m^2$. Second, the heating rate by the level of irradiance. It was found that the level of irradiance affects the cell temperature of both the Polymer-F-White and Polymer-F-Black modules with the similar rate of 0.0270 $°C/(Wm^{-2})$ compared to 0.0268 $°C/(Wm^{-2})$. Finally, the SWA cell temperature over the period of 1 June till 30 September was evaluated from the measured data. The hypothesis was that the modules with a black backsheet would measure higher cell temperatures since black surfaces absorb more heat than any color. Nevertheless, the SWA cell temperature was found to be comparable as well. The SWA cell temperature for the Polymer-F-White modules was, [38.3 - 38.7]$°C$, compared to the Polymer-F-Black modules, [38.1 - 38.7]$°C$. The results present comparable cell temperatures and show no influence of backsheet color on the cell temeprature.

The second comparison was made regarding the electrical performance of the modules. First the energy yield (EY) was measured over the period of 1 June till 30 September. It was found to be 1.54% higher for Polymer-F-White modules compared to the Polymer-F-Black modules. Second, the daily performance ratio (PR) was measured over the period of 1 June till 30 September. It was found that the Polymer-F-White modules had a higher daily PR, [87.7 - 89.1]%, compared to the Polymer-F-Black modules, [86.8 - 87.8]%. The separate analysis of MPP current and MPP voltage allowed to find optical and thermal influence on the performance of the modules. After normalising current and voltage with the indoor I-V measurement STC values, the modules were able to be compared. fig. 4.19 presented a normalised current difference where just one Polymer-F-White module showed a maximum of 2% higher normalised current compared to all other modules. Since the higher normalised current was just measured for one Polymer-F-White module, the measured current of both Polymer-F-White modules could deviated because of measurement uncertainty. In case of normalised voltage the difference for all modules were negligible. The negligible difference in normalised voltage between Polymer-F-White modules and Polymer-F-Black modules is a result of the comparable cell temperatures. Based on the executed analysis, it can be concluded that Polymer-F-White modules and Polymer-F-Black modules present comparable thermal behaviour, resulting in comparable electrical performance.

5.2. Discussion

In this section, discussion about current- and future research are presented. These points are either needed to be discussed or could not be explored within the duration of this thesis project due to the limited time available.

Firstly, the performance difference measured in the Polymer-H and Glass-H comparison, was not only due to difference in the operating temperature. The normalised current showed a difference between Polymer-H and Glass-H modules that can be related to optical losses. Optical losses such as reflectance, transmittance, angle-of-incidence and other optical related influences. Therefore, future research in the optical behaviour of the polymer modules is recommended.

Secondly, the increased cell temperatures for the polymer-H modules compared to glass-H modules origins from the different materials of the modules. However, thermal properties of the polymer materials are unknown. Thermal modelling could possibly lead the thermal properties of the front- and backsheet. Future research with the focus on finding the thermal properties, like thermal capacity and thermal conductivity, of the backsheet is recommended.

Thirdly, the characterization of the PV modules during indoor I-V measurement caused within this thesis project uncertainty about the trustability of the measured values. Therefore, outdoor STC characterization had to be done, to validate the the indoor measured characteristics. It is recommended for future work, to perform indoor I-V measurements that can be trusted, such that more time is left for the rest of the research objectives.

Finally, the collected data from the experimental setup showed some deviations and uncertainties. The biggest uncertainty in the data was created by the random electrical measurement of the Solaredge Power optimizer. The random time stamp of the measured electrical data lead to the need of interpolated weather data. When the time stamp of electrical data and weather data are alligned, more accurate analysis can be executed. The second big source of uncertainty is related to the cable losses. The focus of the research was on the electrical performance of the PV modules alone. The length of the cables created resistive lossed that reduced the value of the measured power. It is therefore recommended for future research, to reduced the length of the cables significantly. The third source of uncertainty comes from the temperature sensors. modules with just two sensors had the possibility that one of the sensors was not functioning well compared to the other. When three sensors are used, this could give more clarity.

Bibliography

[1] IEA. *Renewables 2021 – analysis*. Dec. 2021. URL: https://www.iea.org/reports/renewables-2021.

[2] *Nationaal Solar trendrapport 2022*. 2022. URL: https://www.solarsolutions.nl/trendrapport/.

[3] SYSTEMIQ and EversPartners. *Constructieve Beperkingen voor Zon-op-Dak in Utiliteitsbouw Eindrapportage*. Nov. 2021. URL: https://www.topsectorenergie.nl/agenda/webinar-constructieve-beperkingen-voor-zon-op-dak-utiliteitsbouw.

[4] HyET Solar. *HyET Powerfoil Flexible light weight solar modules*. 2020. URL: https://www.hyetsolar.com/upload_directory/files/HyET-solar-flyer-powerfoil-roofs-20200101.pdf.

[5] Min-Joon Park et al. "Optimization of Shingled-Type Lightweight Glass-Free Solar Modules for Building Integrated Photovoltaics". In: *Applied Sciences* 12.10 (2022). ISSN: 2076-3417. DOI: 10.3390/app12105011. URL: https://www.mdpi.com/2076-3417/12/10/5011.

[6] Solar Feeds. *Thin-film solar overview: Cost, types, application, efficiency*. Nov. 2020. URL: https://www.solarfeeds.com/mag/wiki/thin-film-solar/.

[7] Solarge. *Over solarge*. n.d. URL: https://solarge.com/over-solarge.

[8] Mardy Huot et al. "Performance Investigation of Tempered Glass-Based Monocrystalline and Polycrystalline Solar Photovoltaic Panels". In: *International Journal of Photoenergy* 2021 (Oct. 2021), pp. 1–8. DOI: 10.1155/2021/2335805.

[9] Green Rhino Energy Ltd. *Solar Glass Mirrors*. n.d. URL: http://www.greenrhinoenergy.com/solar/technologies/solar_glass.php.

[10] DUPONT. n.d. URL: www.tedlar.com.

[11] Engineering Toolbox. *Solids - densities*. 2009. URL: https://www.engineeringtoolbox.com/density-solids-d_1265.html.

[12] SABIC. 2020.

[13] THERMHEX WABEN GMBH. n.d.

[14] Arno Smets et al. *Solar Energy: The physics and engineering of photovoltaic conversion, technologies and systems*. English. UIT Cambridge Limited, 2016. ISBN: 978-1-906860-32-5.

[15] Ali Abdolahzadeh Ziabari. *Photovoltaic thin film solar cells*. n.d. URL: https://asdn.net/asdn/energy/solar.php.

[16] Benning. *Frequently asked questions about curve tracing by means of BENNING PV 2*. n.d. URL: https://www.benning.de/products-en/testing-measuring-and-safety-equipment/measuring-devices-for-photovoltaic/pv-2/faq.html.

[17] F. Ghani et al. "On the influence of temperature on crystalline silicon solar cell characterisation parameters". In: *Solar Energy* 112 (2015), pp. 437–445. ISSN: 0038-092X. DOI: https://doi.org/10.1016/j.solener.2014.12.018. URL: https://www.sciencedirect.com/science/article/pii/S0038092X14006094.

[18] A.D. Dhass, P. Lakshmi, and E. Natarajan. "Investigation of Performance Parameters of Different Photovoltaic Cell Materials using the Lambert-W Function". In: *Energy Procedia* 90 (2016). 5th International Conference on Advances in Energy Research (ICAER) 2015, pp. 566–573. ISSN: 1876-6102. DOI: https://doi.org/10.1016/j.egypro.2016.11.225. URL: https://www.sciencedirect.com/science/article/pii/S1876610216314357.

[19] Arati Joshi, Afrah Khan, and Afra SP. "Comparison of half cut solar cells with standard solar cells". In: *2019 Advances in Science and Engineering Technology International Conferences (ASET)*. 2019, pp. 1–3. DOI: 10.1109/ICASET.2019.8714488.

[20] *PV3x*$_2017_6.3.2_Calculating_DC_Yield-video$. TU Delft, Sept. 2019. URL: https://ocw.tudelft.nl/course-lectures/8-4-2-calculating-dc-yield/.

[21] T. Dierauf et al. “Weather-Corrected Performance Ratio”. In: (Apr. 2013). DOI: 10.2172/1078057. URL: https://www.osti.gov/biblio/1078057.

[22] Anthony F. Mills and Carlos F.M. Coimbra. *Basic heat and mass transfer*. 3E. Temporal Publishing, 2015.

[23] William D. Callister and David G. Rethwisch. *Materials science and engineering: An introduction*. 9th ed. John Wiley and Sons, Inc., 2014.

[24] Zeeshan Hyder. *The Best Solar Panels to buy for your home in 2022*. Apr. 2022. URL: https://www.solarreviews.com/blog/what-are-the-best-solar-panels-to-buy-for-your-home.

[25] Benjamin L. Allsopp et al. “Towards improved cover glasses for photovoltaic devices”. In: *Progress in Photovoltaics: Research and Applications* 28.11 (2020), pp. 1187–1206. DOI: https://doi.org/10.1002/pip.3334. eprint: https://onlinelibrary.wiley.com/doi/pdf/10.1002/pip.3334. URL: https://onlinelibrary.wiley.com/doi/abs/10.1002/pip.3334.

[26] Juan Camilo Ortiz Lizcano et al. “Colored optic filters on c-Si IBC solar cells for building integrated photovoltaic applications”. In: *Progress in Photovoltaics: Research and Applications* 30.4 (2022), pp. 401–435. DOI: https://doi.org/10.1002/pip.3504. eprint: https://onlinelibrary.wiley.com/doi/pdf/10.1002/pip.3504. URL: https://onlinelibrary.wiley.com/doi/abs/10.1002/pip.3504.

[27] Benjamin L. Allsopp et al. “Towards improved cover glasses for photovoltaic devices”. In: *Progress in Photovoltaics: Research and Applications* 28.11 (2020), pp. 1187–1206. DOI: https://doi.org/10.1002/pip.3334. URL: https://onlinelibrary.wiley.com/doi/abs/10.1002/pip.3334.

[28] Evocells. n.d. URL: https://evocells.be/fabrication-photovoltaique-evocells/photovoltaique-caracteristiques/.

[29] Eko Instruments. n.d. URL: https://www.alphaomega-electronics.com/en/2606-pyranometer.html.

[30] Sam Kirchner. *Temperature sensors - Thermistors vs Thermocouples*. Dec. 2020. URL: https://www.ametherm.com/blog/thermistors/temperature-sensors-thermistors-vs-thermocouples.

[31] Atse Louwen et al. “Comprehensive characterisation and analysis of PV module performance under real operating conditions”. In: *Progress in Photovoltaics: Research and Applications* 25.3 (2017), pp. 218–232. DOI: https://doi.org/10.1002/pip.2848. eprint: https://onlinelibrary.wiley.com/doi/pdf/10.1002/pip.2848. URL: https://onlinelibrary.wiley.com/doi/abs/10.1002/pip.2848.

[32] Basant Raj Paudyal and Anne Gerd Imenes. “Investigation of temperature coefficients of PV modules through field measured data”. In: *Solar Energy* 224 (2021), pp. 425–439. ISSN: 0038-092X. DOI: https://doi.org/10.1016/j.solener.2021.06.013. URL: https://www.sciencedirect.com/science/article/pii/S0038092X21004837.

[33] Elettro Brescia. *H1Z2Z2-K - elettrobrescia.it*. Feb. 2019. URL: https://www.elettrobrescia.it/uploads/products/552_tds-552-h1z2z2-k-eng.pdf.

[34] Gabi Friesen et al. May 2018. URL: https://iea-pvps.org/wp-content/uploads/2020/01/Photovoltaic_Module_Energy_Yield_Measurements_Existing_Approaches_and_Best_Practice_by_Task_13.pdf.

[35] Saul Mcleod. *Box plots (also known as box and Whister plots)*. July 2019. URL: https://www.simplypsychology.org/boxplots.html.

A

Extra performance results

This table shows the solar weighted cell temperature which is the cell temperature minus the ambient

A.1. Solar Weighted Average cell temperature minus ambient temperature

Table A.1: Solar weighted delta cell temperatures on the specific days

Days	SHC 3 [$^{\circ}C$]	SHC 4 [$^{\circ}C$]	SHC [$^{\circ}C$]	GHC 3 [$^{\circ}C$]	GHC 4 [$^{\circ}C$]	GHC [$^{\circ}C$]	Δ SHC/GHC [$^{\circ}C$]	Δ SHC/GHC [%]
14 June	24.3	24.7	24.5	22.3	21.8	22.0	2.5	11.4
19 July	19.2	19.7	19.4	18.0	16.3	17.2	2.2	12.8
8 June	3.3	3.3	3.3	2.9	2.9	2.9	0.4	13.8
26 August	5.7	5.6	5.7	4.3	5.4	4.9	0.8	16.3

A.2. Data misalignment

The weather data and cell temperatures were measured, by TNO, every minute at 00 seconds. However, the Solaredge optimizers measurd the electrical data at random minutes and random seconds.

Time	G_POA	PBB_1	PBB_2	PWB_1	PWB_2	PS_HC_3	PS_HC_4	PG_HC_3	PG_HC_4
14:08:00	1151		311		319				
14:09:00	999	270							355
14:10:00	1158								
14:11:00	1134			338			376		
14:12:00	1185					368			
14:13:00	1174								
14:14:00	1174				192				
14:15:00	410							93.1	
14:16:00	270		72.1	74.8		88.8	83.9		85.4

Time	BB_1	BB_2	WB_1	WB_2	S_HC_3	S_HC_4	G_HC_3	G_HC_4
14:08:05				319				
14:08:34		311						
14:09:13	270							
14:09:26								355
14:11:28								
14:11:43						376		
14:11:46			338					
14:12:17					368			
14:14:51				192				

Figure A.1: Time stamps of measured data

A.3. Cable loss calculation

Power points were measured during irradiance level or $1000W/m^2 \pm 5W/m^2$

Table A.2: Cable loss calculation

Module name	P_{STC} [W]	I_{mpp} [A]	P_{loss} (2 cables) [W]	P_{STC} - P_{loss} [W]	P_{STC} reduction [%]
P_wb1	355.1	8.86	11.99	343.11	-3
P_wb2	355.7	8.86	11.99	343.71	-3
P_bb1	353.6	8.78	11.77	341.83	-3
P_bb2	353.1	8.79	11.80	341.30	-3
P_shc3	404.4	11.85	21.44	382.96	-5
P_shc4	404.4	11.87	21.52	382.89	-5
P_ghc3	385.3	12.61	24.28	361.02	-6
P_ghc4	388.7	12.67	24.51	364.19	-6

A.4. Outdoor stc power measurement

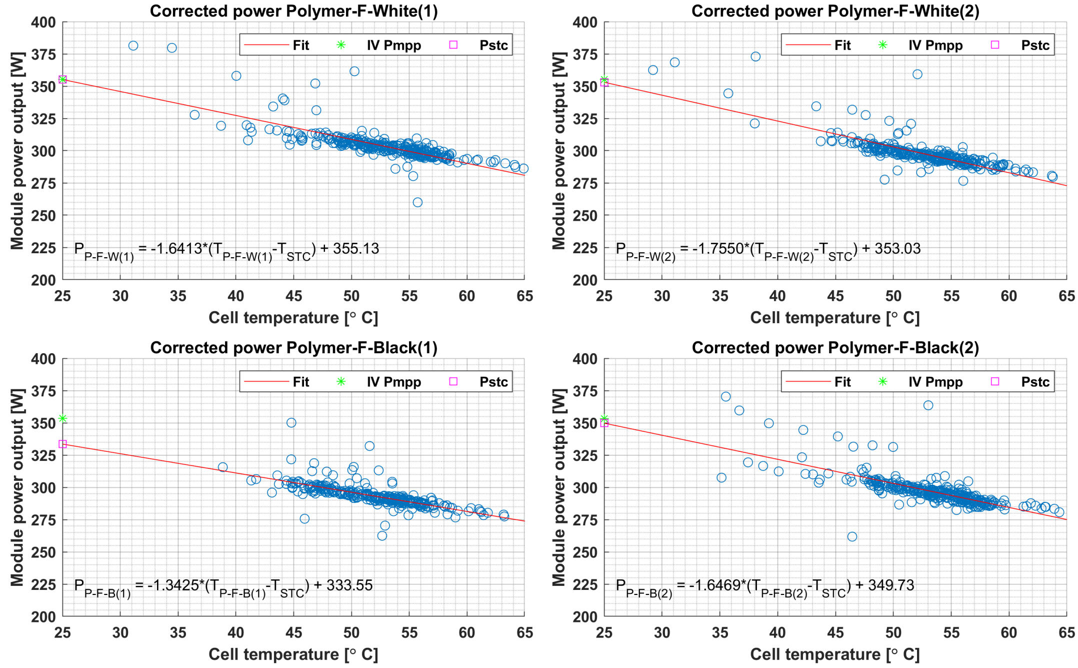

Figure A.2: Outdoor stc power white- and black backsheet solarge modules

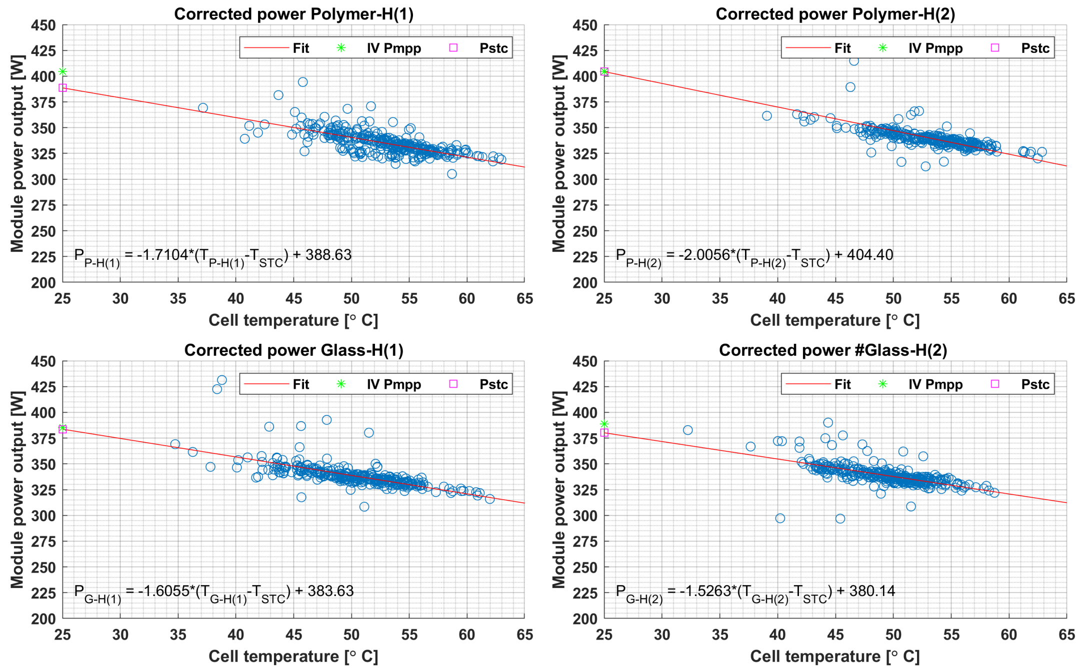

Figure A.3: Outdoor stc power half-cut cell solarge modules and conventional glass modules

B

Statistics and Uncertainty

B.1. Box plot

In chapter 4, box plots were used to give a number to the performance ratio over a period. Box plots are used in statistics for the visualisation of data analysis.

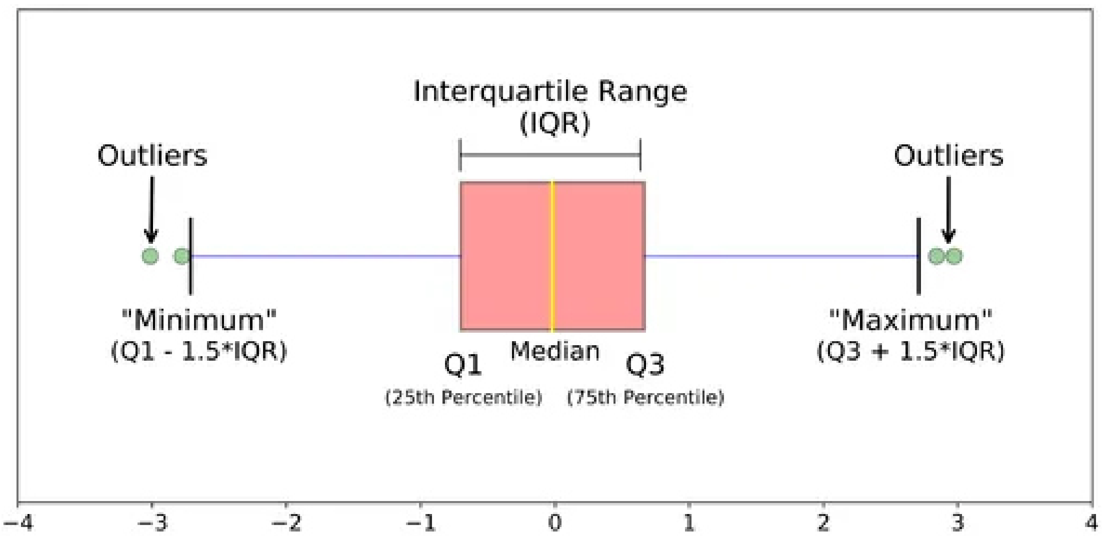

Figure B.1: Boxplot theory [35]

Figure B.1 displays an example of the box plot, as used in this report. The details of the boxplot are explained as followed[35]:

- **Box(red):** The box, also called interquartile range, represents 50% of the datapoints ranging from Q1 to Q3.
- **Whiskers:** The two lines outside the box represents each 25% of the datapoints and are called whiskers.
- **Minimum:** The lowest point in the dataset excluding outliers.
- **Q1:** this is called the lower quartile where 25% of the data is below this value and 75% is above this value.
- **Median:** this is the value in the middle of the dataset. This is exactly at 50%.
- **Q3:** this is called the upper quartile where 25% of the data is above this value and 75% is below this value.
- **Maximum:** The highest point in the dataset excluding outliers.
- **Outliers:** this represents datapoints that are distant from the the dataset and fall outside the boundaries of the whiskers. Therefore, the outliers are marked away from the whisker.

C
Datasheet Evocells

MADE IN BELGIUM

evocells
PHOTOVOLTAÏQUE
MADE IN BELGIUM

Evocells Performance

"Technology and performance"

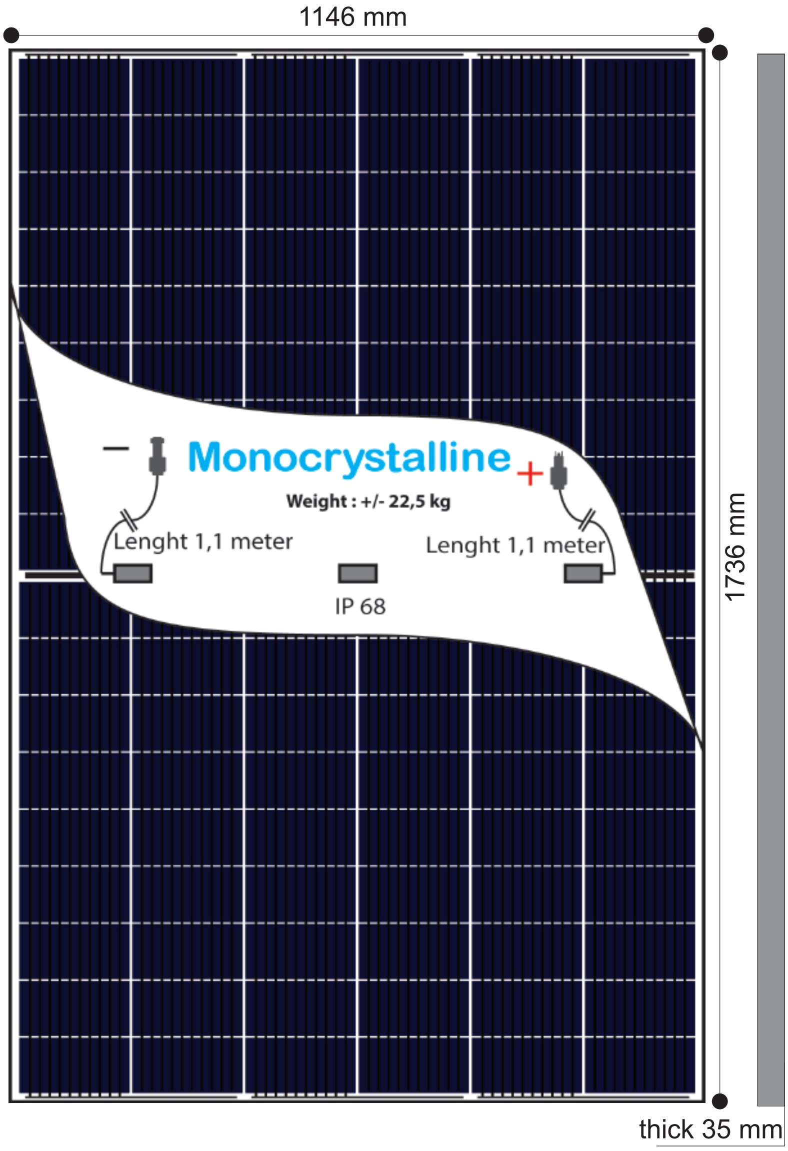

Electrical Specifications

		Positive tolerance range 0/+5Wc		
Pmax	(Wc)	400	405	410
Umpp	(V)	31,42	31,72	31,93
Uoc	(V)	37,98	38,03	38,09
Isc	(A)	13,40	13,45	13,50
Impp	(A)	12,73	12,77	12,84

Technical characteristics

Glass	Anti-reflective Tempered	3,2 mm
Frame	anodized aluminum	Black
Backsheet		PET - coated White
Junction box		IP68
Bypass diodes - 18A		3

Limit values

Max system voltage	1000 V DC
NOCT	45 C° +/-2
Maximum load	2400 N/m

Temperature coefficients

Pmpp	-0,390 %/c°
Temperature coefficient Uoc	-0,300 %/c°
Temperature coefficient Isc	0,060 %/c°

Certifications and guarantees

IEC 61215 : 2016 & IEC 61730 : 2016	
European production - Factory inspection	
Mechanical warranty	20 ans
90% linear Pmax warranty	15 ans
80% Pmax warranty	25 ans
Electroluminescence - Test in our factory in Belgium	100 %
Carbone footprint	ZERO
CO2 Strategy certificat	nr 190601

Values in STC conditions: radiation 1000W/m², AM 1,5 and t° cell of 25 c°

NEW PHOTOVOLTAIC PANEL :

The first european solar panel with the half cut Cells 182 mm

CE PV CYCLE

CARBON NEUTRAL CO2Strategy.be certified EVOCELLS - CERT NR 190601

Our production site

www.evocells.be

Zone d'activités Nord, 89 - B5377 BAILLONVILLE
TEL. 086/38.81.38 - info@evocells.be